arXiv:2009.05712v1 [astro-ph.GA] 12 Sep 2020

Comparisons of Different Fitting Methods for the Physical Parameters of A Star Cluster Sample of M33 with Spectroscopy and Photometry

Zhou Fan[1], Bingqiu Chen[2], Xiaoying Pang[3],Juanjuan Ren[1], Song Wang[1], Jing Wang[1,4], Kefeng Tan[1], Nan Song[1], Chun Li[1], Jie Zheng[1], Gang Zhao[1,4]

zfan@bao.ac.cn

ABSTRACT

Star clusters are good tracers for formation and evolution of galaxies. We compared different fitting methods by using spectra (or by combining photometry) to determine the physical parameters. We choose a sample of 17 star clusters in M33, which previously lacked spectroscopic observations. The low-resolution spectra were taken with the Xinglong 2.16-m reflector of NAOC. The photometry used in the fitting includes u_{SC} and v_{SAGE} bands from the SAGE survey, as well as the published $UBVRI$ and $ugriz$ photometry. We firstly derived ages and metallicities with the ULySS (Vazdekis et al. and PEGASE-HR) SSP model and the Bruzual & Charlot (2003) (BC03) stellar population synthesis models for the full-spectrum fitting. The fitting results of both the BC03 and ULySS models seem consistent with those of previous works as well. Then we add the SAGE u_{SC} and v_{SAGE} photometry in the spectroscopic fitting with the BC03 models. It seems the results become much better, especially for the Padova 2000+Chabrier IMF set. Finally we add more photometry data, $UBVRI$ and $ugriz$, in the fitting and we found that the results do not improve significantly. Therefore, we conclude that the photometry is useful for improving the fitting results, especially for the blue bands ($\lambda < 4000$ Å), e.g., u_{SC} and v_{SAGE} band. At last, we

[1]CAS Key Laboratory of Optical Astronomy, National Astronomical Observatories, Chinese Academy of Sciences, Beijing 100101, China

[2]South-Western Institute For Astronomy Research, Yunnan University, Chenggong District, Kunming 650500, China

[3]Xi'an Jiaotong-Liverpool University, 111 Ren'ai Road Suzhou Industrial Park, Suzhou, Jiangsu Province, 215123, China

[4]School of Astronomy and Space Science, University of Chinese Academy of Sciences, Beijing 100049, China

discuss the "UV-excess" for the star clusters and we find five star clusters have UV-excess, based on the *GALEX* FUV, NUV photometry.

Subject headings: galaxies: individual (M31) — galaxies: star clusters — globular clusters: general — star clusters: general

1. Introduction

Over the last decades, study of the Local Group (LG) has become more and more important and exciting as near-field cosmology and galactic archeology have made great achievements. One of the most important discoveries is confirmation of the future collision and merger of Andromeda (M31) and the Milky Way (MW) from *Hubble Space Telescope* (*HST*) data (see, e.g., van der Marel et al. 2012), and the latest results including Gaia's DR2 data (van der Marel et al. 2019). In addition, the Pan Andromeda Archeological Survey (PAndAS) (McConnachie et al. 2009) discovered a large number of stellar streams and substructures in the M31 halo. Numerous giant stellar streams (e.g., northwest stream, Richardson et al. 2011) and substructures have been discovered. With deep observations of the Canada Canada-France-Hawaii Telescope (CFHT) $g = 26.0$ and $i = 24.8$), the furthest streams are located up to $\sim$ 150 kpc from the M31 center (Mackey et al. 2019). A large number of star clusters and dwarf galaxies have also been discovered in the halo of M31 up to 150 kpc. Recently, Mackey et al. (2019) systematically investigated the density map of M31 with PAndAS. They found a relation between the bright substructures in the metal-poor halo field and positions of star clusters. At the same time, M31 has been having strong interactions with M33 since 3.4 Gyr ago (McConnachie et al. 2009). Therefore, study of star cluster systems associated with M33 is also important for the interaction and evolution of the M31-M33 system.

The integrated light (IL) spectroscopy is a useful and powerful tool for the analysis of star clusters in extra-galaxies. The astrophysical parameters, e.g., ages, chemical abundances (including the [α/Fe]), velocities and masses can be derived with the stellar synthesis models, which provide crucial information about their host galaxies (Sakari 2019). If the halo star clusters are spatially related to the star stream or substructures of M31, the study of these halo star clusters can reveal information about the nature of interactions between M31 and M33. Fan & Yang (2014) described how to trace the substructures and the interaction of M31-M33 with the associated star clusters via spectroscopic observations of the Xinglong 2.16-m telescope (Fan et al. 2011, 2012) and the Multiple Mirror Telescope (MMT) 6.5-m telescopes (Fan et al. 2016a). The studies of Chen et al. (2015, 2016) derived stellar parameters (e.g., radial velocities, ages, metallicities, and masses) for star clusters in M31, using

the LAMOST (Large sky Area Multi-Object fiber Spectroscopic Telescope) low-resolution spectroscopic survey with R$\sim$ 1800 from 3700 Å to 9100 Å in wavelength (Zhao et al. 2012; Cui et al. 2012).

Many different spectroscopic fitting techniques have been developed to increase the accuracy of parameters derivation. One of these involves full-spectral fitting, e.g., using ULySS (Koleva et al. 2009; Chen et al. 2016). Alternatively, one could pursue $\chi^2_{\rm min}$ fitting of various Lick/IDS indices (e.g., Fan et al. 2011, 2012; Chen et al. 2016). Note that the results and precision are model-dependent. Inclusion of more useful information obviously leads to higher precision. Therefore, $\chi^2_{\rm min}$ fitting combined with SED and Lick-index fitting is expected to provide more reliable and higher-precision results than any of the individual approaches (Fan et al. 2016a). Lilly et al. (2009) have also done similar work for the globular cluster systems of NGC5128 and they found a population of intermediate age and metal-poor clusters for the first time.

On the other hand, the $\chi^2_{\rm min}$ SED-fitting of globular clusters' spectral energy distributions (SEDs) is another efficient method to determine the parameters on the basis of multi-passband photometry/imaging data. de Grijs et al. (2003) derive the ages, metallicities, and reddening of the star clusters associated with NGC 3310 by the SED-fitting method with the photometry of the ultraviolet (UV), optical, and near-infrared (NIR) observations obtained with the HST. Fan et al. (2006); Ma et al. (2007, 2009, 2011, 2012); Wang et al. (2010, 2012) have done a series of SED-fitting works targeting M31 star clusters, based on the Beijing–Arizona–Taiwan–Connecticut (BATC) multi-color photometry system, with a 60/90cm Schmidt telescope. They applied the simple stellar population (SSP) models, Bruzual & Charlot (2003, henceforth BC03) and the Galaxy Evolutionary Synthesis Models (*GALEV*; Lilly & Fritze-v. Alvensleben 2006; Kotulla et al. 2009). To achieve a higher precision, they make use of multi-band photometry, such as the broad-band $UBVRI$ filters, JHK bands from the Two Micron All Sky Survey (2MASS), the near-UV (NUV) and far-UV (FUV) channels of the Galaxy Evolution Explorer (*GALEX*), as well as the $ugriz$ bands of the Sloan Digital Sky Survey (SDSS).

The recent SAGE (Stellar Abundances and Galactic Evolution) survey (PI: Gang Zhao , see, e.g., Fan et al. 2018; Zheng et al. 2018, 2019a,b) covers 12,000 deg^2 of the northern sky with eight photometric bands. Its $v_{\rm SAGE}$ filter is self-designed. The project will present one of the largest catalogs of (a few hundred million) stars with available stellar atmospheric parameters. The $u_{\rm SC}$, $v_{\rm SAGE}$ photometry is sensitive to the metallicity [Fe/H] and surface gravity $\log g$, Thus far, the observations of $u_{\rm SC}$, $v_{\rm SAGE}$, gri-bands have almost been completed. The data can be used to derive the age and metallicity of the stellar populations in M31/M33, as well as precise interstellar extinctions.

Theoretically, spectroscopy provides much more information than the corresponding photometry. However, in many cases, the precision of the spectral flux calibration is much lower than that of photometry, especially for the blue bands (e.g., $\lambda < 4000$ Å) in some cases, for the limit of observing condition. Thus the photometry could be quite useful for improving the precision of the flux calibration of the spectra. Given that the wavelength coverage of the spectrum is not wide enough, especially for blue bands, the photometry seems much more important and can be served as a complement for the spectroscopy.

In our work, we derive the ages and metallicities of our M33 star cluster samples with different fitting methods based on the spectra and photometric data. The spectra were taken from the BFSOC spectrograph on the Xinglong 2.16-m telescope, while the photometric data are from the SAGE survey in u_{SC}, v_{SAGE} bands, and the literature in $UBVRI$ and $ugriz$ bands. For comparison, both the ULySS models and BC03 models have been applied in the fitting. The organization of the paper is as follows. In Section 2, we describe the selection of sample and introduce the methods adopted for the fits. In Section 3 we describe the observation details for both 2.16-m telescope of Xinglong as well as that of the SAGE survey; In Section 4 the full-spectrum fitting is described, which provides the best-fitting results compared to the ULySS models and the Bruzual & Charlot (2003) models; in Section 5, we introduce the fitting process of the Spectrum-SED fitting, based on $\chi^2_{\rm min}$ fitting with Padova 1994/2000 evolutionary tracks and Chabrier (2003)/ Salpeter (1955) IMFS of the BC03 models; different data sets have been fitted separately; in Section 6, we compare the *GALEX* FUV/NUV data with the SAGE u_{SC} and the Johnson-Cousins U-band, and found some UV excess candidates. Finally, the summary and concluding remarks are given in Section 7.

2. The Selection of Star Cluster Sample in M33

M33 (Triangulum Galaxy) is the third largest spiral galaxy in our Local Group (LG). The distance of M33 from us is 847 ± 60 kpc, which corresponds to a distance modulus of $(m - M)_0 = 24.64 \pm 0.15$ mag (Galleti et al. 2004). The sources were selected from Table 3 of Sarajedini & Mancone (2007), which contains 451 star cluster candidates in M33. In this work, we select 17 confirmed and luminous clusters ($V < 17.5$) as our sample, which is suitable for spectroscopic observations with a 2-meter class telescope. These star clusters lack spectroscopic observational data, especially the metallicity measurements. Thus, it is necessary to observe the spectra of these sample clusters systematically and constrain the spectroscopic metallicities and ages in detail.

The observational information of our sample star clusters is listed in Table 1, which

includes the IDs, which are the same as Sarajedini & Mancone (2007), coordinates, observation dates and exposures. All the coordinates (R.A. and Dec. in Cols. 2 and 3) are from Sarajedini & Mancone (2007) . The star clusters are sorted by V-mag.

Figure 1 shows the spatial distribution of the sample star clusters (green circles) in M33. Cluster names are in Table 1. The images are from SAGE v_{SAGE}-band observations with the Bok 2.3-m (90-inch) telescope of Steward Observatory, University of Arizona. A four 4k×4k blue sensitive CCD mosaic is mounted and for each CCD there are four amplifiers. The field of view (FoV) is ~ 1 deg^2.

3. The Spectroscopic Observations and Data Reduction

The low-resolution spectroscopic observations were carried out in 2015 with the Xinglong 2.16-m reflector (Fan et al. 2016b) Beijing Faint Object Spectrograph and Camera (BFOSC) instrument during October 9 to 11, and October 19. The telescope is located in Xinglong Observatory, National Astronomical Observatories, Chinese Academy of Sciences (NAOC), in Hebei Province at an altitude of ∼900 m. Most clusters are exposed for 3600 seconds except for SM197 (4200 seconds) due to weather conditions (Table 1). The seeing was $\sim 2''$ to 3". We adopted a slit with a width of 1.8", with the grism G4. The first order dispersion is 4.45Å pixel^{-1} and the wavelength coverage is 38507000Å. The spectral resolution was $R = 620$ for slit of $0.6''$ and a central wavelength of 5007Å (Fan et al. 2016b). The E2V 55301348 back-illuminated 1242×1152 pixels^2 CCD, AIMO was installed. The pixel size is 22.5 μm and pixel scale is $0''.457$. The gain is 1.08 e$^-$ ADU^{-1}, with a readout noise (RN) of 2.54 e$^-$. The FOV is $9'.46 \times 8'.77$ according to the size of the CCD and the maximum QE is higher than 90% around 5700 Å of the wavelength.

The data reduction follows the standard procedures with the NOAO Image Reduction and Analysis Facility (IRAF v.2.15) software package. After carefully checking the spectral images by eye, we perform the bias combinations with `zerocombine` and bias corrections with `ccdproc`, the flat-field combination, normalization, and corrections with `flatcombine`, `response`, and `ccdproc`. Cosmic rays are eliminated with the package `cosmicrays`. The star cluster spectra and comparison arc lamp spectra are extracted with `apall`. The wavelength calibrations are performed with helium/argon-lamp spectra, which were taken at the beginning and end of each observing night. The spectral features of the comparison lamps are identified with `identify`. The wavelength is calibrated with the package `refspectra`. Then `dispcor` is used for the dispersion correction and to resample the spectra. We use four Kitt Peak National Observatory (KPNO) spectral standard stars in Massey et al. (1988) for flux calibrations. The `standard` and `sensfunc` packages are used to combine the standard stars

and determine the sensitivity and extinction of the atmosphere. In the last step, we apply the `calibrate` package to correct the atmospheric extinction and finish the flux calibration.

We display the normalized, calibrated spectra of our sample star clusters in Figure 2, with their names indicated (taken from Sarajedini & Mancone (2007)). Note that the emission lines of night sky [OI] are at 5577Å and the oxygen absorption lines of Earth's atmosphere are around 7600 Å. The signal-to-noise ratios (SNRs) of most clusters are high enough, except for the star clusters SM 243 and 245.

4. The Full-Spectrum-fit with ULySS and BC03 Models

In order to compare the fitting results, we also adopt the ULySS (Koleva et al. 2009) models for the full spectral fitting to derive the ages and metallicities of star clusters. The Vazdekis et al. (2010) SSP models cover the wavelength ranges of 3540.5Å – 7409.6Å at a full width at half maximum (FWHM) of 2.3Å. The models are based on the MILES (Medium-resolution INT Library of Empirical Spectra) spectral library (Sánchez-Blázquez et al. 2006). The stellar initial mass function (IMF) of Salpeter (1955) is adopted for the fitting and the solar-scaled theoretical isochrones of Girardi (2000) have been used. The age range is 10^8–1.5×10^{10} yr and the metallicity is [Fe/H] = −2.32 dex ($Z = 0.0004$) – +0.22 dex ($Z = 0.03$). Furthermore, another independent SSP model, PEGASE-HR, which is provided by Le Borgne et al. (2004), is based on the empirical spectral library ELODIE (e.g., Prugniel & Soubiran 2001; Prugniel et al. 2007). The wavelength coverage is 3900Å – 6800Å with a spectral resolution $R \sim 10,000$. In this model, the fitted stellar atmospheric parameters are effective temperature, $T_{\rm eff}$ (3100–50,000 K), gravity $log\ g$ (−0.25 dex – 4.9 dex), and metallicity [Fe/H] (−3 dex – +1 dex). The flux calibration accuracy is 0.5–2.5%. We adopt the PEGASE-HR SSP models with the Salpeter (1955) IMF. The age ranges from 10^7 to 1.5×10^{10} yr, and the metallicity [Fe/H] = −2.0 dex ($Z = 0.0004$) to +0.4 dex ($Z = 0.05$).

Table 2 lists the ages and metallicities derived from the full-spectrum fitting with ULySS including Vazdekis et al. (2010) and PEGASE-HR SSP models. The errors are calculated from Monte-Carlo simulations, which are performed to estimate the biases, errors and coupling (degeneracies) between the parameters. For the fitting, a series of random errors are added in the data and then the resulting the errors. From Table 2 we can see that most of the star clusters are younger than 2 Gyr, except for SM 197, 402 and 206. There is a discrepancy in the age of SM 243, which is 1.48 Gyr from the Vazdekis et al. (2010) model, but 10.72 Gyr from PEGASE-HR. We note that the χ^2/dof for this source is relatively large, 2.27 and 2.96 for the two models, which may be the reason for the discrepancy in age. If we consider it to be the old population, then 13/17-14/17 (76.5%-82.3%) of the sample is the young star

clusters, which agrees with the previous conclusions that the young star clusters dominate in M33. On the other hand, the Vazdekis et al. (2010) SSP model tends to result in a lower metallicity than PEGASE-HR, more than (or almost) 1 dex, e.g., SM198, 371, 140, 70, 228, 221 and 85. Meanwhile, it is noted that the age *log t* of these clusters in Vazdekis et al. (2010) models is basically (at least) $\sim 0.5 - 0.6$ dex older than that of PEGASE-HR models. It may be due to the different spectral libraries applied in the two models: Vazdekis et al. (2010) SSP models cover wider wavelength ranges and smaller metallicity lower-limit than PEGASE-HR; PEGASE-HR SSP models extend the lower limit of ages to 10^7 yr, which is one order of magnitude smaller than that of Vazdekis et al. (2010). In order to make it clear, we plot Figure 3 to show the differences in the parameters derived from the two models. Apparently it is affected by the age-metallicity degeneracy, which can usually be found in the SED fitting.

Since there are many previous works for determining the ages and metallicities of M33 star clusters, it is necessary to compare if there are sources in common. Regarding spectroscopy, for instance, Beasley et al. (2015) provided both age and metallicities based on the observations of Gran Telescopio Canarias (GTC) and William Herschel Telescope (WHT). Schommer et al. (1991) only provide the velocities and did not provide the age and metallicities. Chandar et al. (2002) only reported the velocities and ages, but no metallicity information. Chandar et al. (2006) did not provide the catalog for age and metallicity. Sharina et al. (2010) have only one star cluster in common with our work, CBF129 (SM228 in our work), age $t = 1.5$ Gyr and [Fe/H] $= -1.7$ dex and we have added it to our comparisons. For the photometry, Fan et al. (2014) used the SED-fitting with the photometry in UBVRI/ugriz and JHK bands if available, which is the most comprehensive, updated and homogeneous sample. Thus we only adopted the literature from Beasley et al. (2015), Fan et al. (2014) and Sharina et al. (2010). Figure 4 shows the comparisons between the results from full-spectrum method of Vazdekis et al. (2010) and PEGASE-HR models and that from Beasley et al. (2015), Fan et al. (2014) and Sharina et al. (2010). As shown in the figure, the offsets (median difference) are quite small for both the ages (-0.14 and -0.06), with scatters of (0.68 and 0.78 for the Vazdekis et al. (2010) and PEGASE-HR models respectively. The offsets of metallicities [Fe/H] and the references are -0.12 and -0.21 dex, with scatters of 0.70 and 1.16. It can be seen that the ages from both models are comparable, although the offset of the Vazdekis et al. (2010) model and the references are smaller, but the scatter is slightly larger. The largest difference is SM 402, for which Fan et al. (2014) gives 1.26 Gyr, but the result from Beasley et al. (2015) is 11.74 Gyr. In our full-spectrum fitting with ULySS model, the results are also old, 11.22 Gyr in the Vazdekis et al. (2010) model and 13.49 Gyr in the PEGASE-HR model. Since both the results from Beasley et al. (2015) and our work are derived from spectroscopy, which contains more information than the photometry in Fan et al.

(2014), we believe our results are more reliable. On the other hand, it is known that the models are not sensitive to the ages $> 1 - 2$ Gyr for the BC03 SSP models, especially for the SED-fit.

Similarly, we have performed the full-spectrum fitting with the Bruzual & Charlot (2003) models. The evolutionary stellar population synthesis models of Bruzual & Charlot (2003, hereafter BC03) not only provide spectra and SEDs for different physical parameters, but also Lick/IDS absorption-line indices. The models adopt Padova 1994 and Padova 2000 stellar evolutionary tracks, with initial mass functions (IMFs) of Salpeter (1955) and Chabrier (2003). The wavelength coverage ranges from 91 Å to 160 μm. The Padova 1994 model offers six metallicity options ($Z = 0.0001$, 0.0004, 0.004, 0.008, 0.02, and 0.05), and the Padova 2000 model also offers six ($Z = 0.0004$, 0.001, 0.004, 0.008, 0.019, and 0.03). In total, there are 221 age steps from 0 to 20 Gyr. In our work, we adopted both Padova 1994 and Padova 2000 stellar evolutionary tracks for the purpose of comparison. However, since there are only six metallicity values in the model, which seems not enough for the fitting, we interpolate the metallicities to 61 values. Thus the fitting results can be more smooth and better distributed.

We show our fitting results in Table 3 and Table 4, which list the ages and metallicities derived from the full-spectrum fitting with Bruzual & Charlot (2003) SSP models, with Padova 1994 and Padova 2000 evolutionary tracks respectively. In each case, we use the Chabrier (2003) and Salpeter (1955) IMFs, separately. It is easy to find that for SM 402 and 206, which are old in Table 2, they are also old in fitting with BC03 models. However, for SM 197 and 243, the results of BC03 models are much younger than those from the ULySS model. Figure 5 and Figure 6 are similar comparisons of the fitting results with the literature of Beasley et al. (2015), Fan et al. (2014) and Sharina et al. (2010). We find that for the ages, the offset from the Padova 2000 evolutionary track with Salpeter (1955) IMF is 0.02, which seems much smaller than that from Padova 1994 track (-0.10), except for the comparison with that of models with Chabrier (2003) IMF (offset= -0.38). For the metallicity, median difference from the Padova 2000 track is slightly smaller than that from the Padova 1994 track, although the scatters are comparable. Compared with the ULySS model, for the ages, the median differences of both the Padova 1994 and Padova 2000 tracks are basically comparable, and the scatters are slightly smaller. For the metallicity, although the median difference of Padova 1994 tracks is comparable with that of ULySS fittings, but for the Padova 2000 tracks, the median difference of the fitting results are much smaller, although the scatter is similar.

5. The SAGE Photometry and Spectrum-SED-fit with Models

5.1. Fitting with spectroscopy and the SAGE photometry

Since the M33 galaxy is 847 ± 60 kpc from us, the star clusters are almost the point sources (a little bit extended) for the ground-based telescopes, either for spectroscopy or for the photometry, which guarantee that the data take into account the same stellar population/ same region of one star cluster. As mentioned in Sect. 1, the SAGE survey[5] (PI: Gang Zhao , see, e.g., Fan et al. 2018; Zheng et al. 2018, 2019a,b) has been operating since 2015 and it covers 12,000 deg^2 of the northern sky with declination $\delta > -5^\circ$, excluding the Galactic disk ($|b| < 10^\circ$) which is bright and with high extinction. The survey provides photometry in eight bands u_{SC},v_{SAGE}, g, r, i, Hα_n, Hα_w and DDO51. The central wavelengths of the u_{SC} and v_{SAGE} bands are 3520 and 3950 Å respectively (Fan et al. 2018). The wavelength coverage of blue-band filter usually includes various metallicity absorption lines, e.g., u_{SC}-band. In particular, the v_{SAGE} band covers the CaII K line at $\lambda = 3933.44$ Å (between Hϵ and Hζ), which is very sensitive to metallicity for FGK stars. The observations of the u_{SC} and v_{SAGE} bands are almost completed ($\sim$ 88% so far). Therefore, we utilized the photometry of the two bands to derive the ages, metallicities and interstellar extinctions of our star cluster samples of M33. The observations of these two bands were carried out by the 90-inch (2.3-m) Bok telescope of Steward Observatory, University of Arizona. A CCD mosaic camera, which consists of four 4k×4k CCDs, is mounted at the prime focus. The field of view is 1 deg^2 and the pixel size is 0.45″. The photometry pipeline is based on the SExtractor and MAG_AUTO. For astrometry, the SCAMP has been used. The Position and Proper Motion Extended (PPMX) (Roser et al. 2008) catalog is adopted in our pipeline as the astrometric reference. The detailed description of the pipeline of photometry, astrometry, and flux calibrations could be found in Zheng et al. (2019a,b). The SNR of 100 corresponds to a limiting magnitude of $u_{SC} \sim 16.5$ mag and $v_{SAGE} \sim 15.5$ mag; 5 to $u_{SC} \sim 20$ mag and $v_{SAGE} \sim 19.5$ mag. In our photometric reduction, since star clusters are extended sources, the growth curve has been calculated to perform the aperture corrections for the star clusters in both u_{SC}, v_{SAGE} bands.

The photometry of star clusters is calibrated in the AB system with the convolution of the MILES library and our SAGE filters (please see Table 5). We adopt a value of $E(V-I) = 0.06$ mag as the mean Galactic foreground reddening in the direction of M33 (Sarajedini et al. 2000; San Roman et al. 2009). The extinction A_λ is computed using equations 6-7 in Cardelli et al. (1989). The spectra and u_{SC}, v_{SAGE}-band photometry are fitted

[5]http://sage.sagenaoc.science/ sagesurvey/

simultaneously via the equation as followed,

$$\chi^2_{\rm min} = \min \left[\sum_{i=1}^{n_{Spec}} \left(\frac{m^{\rm obs}_{\lambda_i} - m^{\rm mod}_{\lambda_i}(t, [{\rm Z/H}])}{\sigma_{m,i}} \right)^2 + \sum_{j=1}^{n_{Phot}} \left(\frac{M^{\rm obs}_{\lambda_j} - M^{\rm mod}_{\lambda_j}(t, [{\rm Z/H}])}{\sigma_{M,j}} \right)^2 W_j^2 \right], \quad (1)$$

where $m^{\rm obs}_{\lambda_i}$ is the AB magnitude that is transformed from the dereddened observed spectra; $m^{\rm mod}_{\lambda_i}(t, [{\rm Z/H}])$ is the $i^{\rm th}$ magnitude provided in the stellar population model at an age t and metallicity [Z/H]; similarly $M^{\rm obs}_{\lambda_i}$ represents the observed dereddened magnitude in the $j^{\rm th}$ band; $M^{\rm mod}_{\lambda_j}(t, [{\rm Z/H}])$ is the fitted $j^{\rm th}$ magnitude from the stellar population model at an age t, metallicity [Z/H]; n_{Spec} is the interval number of the wavelength/flux of the spectrum; n_{Phot} is the number of photometric bands, and here it equals to 2; W_j is the weight for the photometry fitting times of the $j^{\rm th}$, which is the bandwidth of the SED relative to the mean wavelength interval of the spectrum in the same wavelength coverage; $W_j = \delta\lambda_{SED,j}/\overline{\delta\lambda_{Spec}}$. W_j is important to the second part of the formula, since it is easy to note that the number of photometric bands n_{Phot} is much smaller than spectroscopic data points n_{Spec}. Thus the two fitting parts for photometry and spectroscopy need to be rescaled and relative weight applied. In our work, the value of W_j is $\sim 50 - 80$, which is the same order of weight for the total χ^2 ($g_{PHO} = 0.1$) in Werle et al. (2019).

We also compute the errors associated with MAG_AUTO with those related to the flux calibration, as

$$\sigma_i^2 = \sigma^2_{{\rm obs},i} + \sigma^2_{{\rm mod},i}, \quad (2)$$

where i represents any of the SAGE $u_{\rm SC}$, $v_{\rm SAGE}$ bands. $\sigma_{\rm obs}$ and $\sigma_{\rm mod}$ correspond to the photometric uncertainties associated with model uncertainties, respectively.

The estimated ages and metallicities with $1-\sigma$ errors of the M33 star clusters are listed in Tables 6 and 7, which are derived from the BC03 models of Padova 1994 and Padova 2000 evolutionary tracks, respectively. We estimate the uncertainty associated with a given parameter by fixing the other parameters to their best values, and vary the parameter of interest. The error is computed as $1-\sigma$ $\chi^2_{\rm min}$, which means we calculate the $1-\sigma$ errors for the parameters (i.e., log t or Z). When the contours of χ^2 resulting from the parameter gives $\chi^2_{0.68} = \chi^2_{\rm min}$+2.3, which corresponds to $1-\sigma$ (significance level = 0.68), the contour $\chi^2_{0.68}$ value defines a region of confidence in the (log t, Z) plane corresponding to the $1-\sigma$ level of significance. A cut along a line of constant metallicity Z is the calculation of χ^2 that defines upper and lower values of log t, corresponding to $\sigma = 1$ for this particular metallicity Z. Meanwhile, the errors for metallicity Z are calculated in the same way (Fan et al. 2011, 2012; Chen et al. 2016). It is found that the fitting results are relatively younger than those of the previous full-spectrum fittings. In Tables 6 for the Padova 1994 tracks, it is found that 10/17 of star clusters are younger than 10 Myr *log* $t < 7$, while in Table 7, the proportion

is much lower, only 4/17 of the sample are younger than 10 Myr $log\ t < 7$ for Padova 2000 tracks. In our sample, SM 402 is the only star cluster which is older than 2 Gyr for both models with Padova 1994 and Padova 2000 evolutionary tracks. It is also noted that SM 206 is relatively older for our sample in the fitting results, which is consistent with the previous fittings.

Figures 7-9 show the spectroscopy and SAGE photometry fitting with the BC03 models, with the Padova 2000 evolutionary track + Chabrier (2003) IMF combination. It can be seen that most spectra and photometry data pints are fitted well except for SM198, for which the model is obviously fainter than the observed spectrum in the red part ($\lambda > 7000$ Å). It may be due to the low SNR in the blue band of the spectrum and also it seems u_{SC} mag is brighter than the model predicted in the blue end of the spectrum.

For a consistency check, we compare our fitted ages and metallicities to the references. For the spectroscopic study of M33 star clusters, Schommer et al. (1991), Chandar et al. (2002), Chandar et al. (2006), Sharina et al. (2010), Beasley et al. (2015) can be found. However, most of the works only focus on the kinematics and ages except for Beasley et al. (2015) and Sharina et al. (2010), who provide both age and metallicity information which can be used for comparison with our work. In fact, Sharina et al. (2010) have only one star cluster in common with our work, CBF129 (SM228 in our work), age $t = 1.5$ Gyr and [Fe/H] $= -1.7$ dex with the full spectrum fitting and Vazdekis (1999) models. Therefore, we use the spectroscopic information from Beasley et al. (2015) and Sharina et al. (2010).

As can be seen, the fitting result agrees with the literatures much better for either ages or metallicities for models of Padova 2000 track (Figure 11) than that of Padova 1994 track (Figure 10): the median differences are much smaller, although the scatters are similar. The reason may be due to that the models of Padova 2000 evolutionary tracks have a new version of stellar spectral library of Girardi (2000), which updated equation of state and low-temperature opacities. Thus the results are more reasonable and reliable than that of models with Padova 1994 tracks.

However, we also found some outliers (significant differences) in the comparison. For instance, result of SM 70 is $4.0 - 4.4$ Myr in Table 6 but it is $0.91 - 1.14$ Gyr in Table 7. For reference, Beasley et al. (2015) provided the age of 1.18 Gyr, and the results of full-spectrum fittings are ~ 1 Gyr for BC03 model fitting (Tables 3 and 4) or several $\times 10^8$ yr for ULySS fittings. Thus we considered it due to the updated stellar spectral library in the models of Padova 2000, which is more reliable.

5.2. Fitting with spectroscopy and the SAGE photometry, UBVRI and ugriz photometry

In this section, we would like to figure out if adding more photometry data can improve the fitting results further. Thus, we have gathered the photometry of our sample star clusters in the u_{SC} (SAGE), v_{SAGE} (SAGE), $UBVRI$ (Mayall) and $ugriz$ (CFHT) bands. The magnitudes of the $UBVRI$ bands are taken from Ma (2013) who carried out the observations by the Mayall 4-m telescope. They transformed the Vega magnitude system to the AB system with $m_{AB} - m_{Vega}$ =0.79, −0.09, 0.02, 0.21 and 0.45 (following: http://www.astronomy.ohio-state.edu/∼martini/usefuldata.html, Blanton et al. 2007). The $ugriz$ magnitudes were obtained with the CFHT 3.6-m telescope and in the AB system (San Roman et al. 2010). The u_{SC}, v_{SAGE} photometry of the SAGE survey in Table 5 is also in the AB system. The photometry taken from published work is listed in Table 8. We adopt a value of $E(V-I) = 0.06$ mag as the mean Galactic foreground reddening in the direction of M33 (Sarajedini et al. 2000; San Roman et al. 2009). The extinction A_λ is computed using equations 6-7 in Cardelli et al. (1989). The spectra and SEDs are fitted simultaneously via the equation as in the following,

$$\chi^2_{\rm min} = \min \left[\sum_{i=1}^{n_{Spec}} \left(\frac{m^{\rm obs}_{\lambda_i} - m^{\rm mod}_{\lambda_i}(t, [{\rm Z/H}])}{\sigma_{m,i}} \right)^2 + \sum_{j=1}^{12} \left(\frac{M^{\rm obs}_{\lambda_j} - M^{\rm mod}_{\lambda_j}(t, [{\rm Z/H}])}{\sigma_{M,j}} \right)^2 W_j^2 \right], \quad (3)$$

where the meanings of all physical quantities are the same as in eq. 1 but the number of photometric bands is 12 in the fitting. Similarly, we compute the errors associated with MAG_AUTO with those related to the flux calibration, as

$$\sigma_i^2 = \sigma^2_{{\rm obs},i} + \sigma^2_{{\rm mod},i}, \quad (4)$$

where i represents any of the SAGE u_{SC}, v_{SAGE}, $ugriz$ magnitudes, and $UBVRI$ bands. $\sigma_{\rm obs}$ and $\sigma_{\rm mod}$ correspond to the photometric uncertainties associated with the respective model uncertainties.

The estimated ages and metallicities with $1-\sigma$ errors of the M33 star clusters are listed in Tables 9 and 10. We estimate the uncertainty associated with a given parameter by fixing the other parameters to their best values, and vary the parameter of interest. The error is computed as $1-\sigma$ $\chi^2_{\rm min}$. We found that again, 8/17-9/17 of star clusters in our sample for that from the Padova 1994 models in Tables 9 are younger than 10 Myr $log\ t < 7$, while in Table 10, the proportion is much lower: only 5/17 of the sample are younger than 10 Myr $log\ t < 7$ for models of Padova 2000 tracks. The proportions of fitting results are similar to those of in Tables 6 and 7. Particularly, in Table 10 with the Chabrier (2003) IMF, the ages of SM 206 is $9.51 - 9.75$ Gyr, which agree with that of Beasley et al. (2015) (9.98

Gyr). While for SM 402, it is $6.75 - 7.74$ Gyr in Table 10 with the Chabrier (2003) IMF, but 11.74 Gyr for Beasley et al. (2015). We consider that the age is not very sensitive for the stellar population when $> 1 - 2$ Gyr in the BC03 SSP models. The fitted models and observational spectra and photometry are plotted in Figures 12-14. It is found that most of star clusters are fitted well except SM198, for which the red part of the spectral seems much redder than the model, but agree with the photometry. As for star cluster SM70, the observed spectrum is not consistent with its SED or the model spectrum, especially in the blue part of the spectrum ($\lambda < 5500$ Å). The fitting result is 6.6 Myr, is much younger than the Beasley et al. (2015) value 1.18 Gyr, and that of full-spectrum fitting (1.14 Gyr, see Table 4) / SAGE+spectrum (1.14 Gyr, see Table 7) with BC03 models. However, the result is relatively closer to that of the PEGASE-HR models of ULySS fittings (79.4 Myr, see Table 2). We have checked the data and found no problem. Further, we also found the photometry in the similar band, $u = 18.01$ mag from San Roman et al. (2010) are 0.5 mag brighter than our photometry $u_{SC} = 18.51$ mag, and $U = 17.56$ mag from Ma (2013) is even ~ 1 mag brighter. If we remove the SAGE u_{SC} band photometry, only leaving u and U mags in $\lambda < 4000$ Å for the photometry, the fitting result could become even younger. Thus we think our photometry u_{SC} dose not account for the disagreement with literature, and probably we may take high S/N spectrum, especially in the blue part ($\lambda < 4000$ Å) in the future work.

For a consistency check, we compare our fitted ages and metallicities to those of Beasley et al. (2015) and Fan et al. (2014) in Figures 15 (with Padova 1994 track) and 16 (with Padova 2000 track). Again, the results of the Padova 2000 track are much better than those of Padova 1994, either for ages or metallicities, which may be due to the updated library of models. As can be seen, in the top panels of Figure 16, the median differences between our fitted ages and the literatures are $\delta\ log\ t = 0.12$, which is slightly larger than that fitted with spectroscopy+SAGE photometry in Figure 11 ($\delta\ log\ t = 0.04 - 0.08$). On the other hand, however, it seems that the fitting errors have been reduced in Figures 15 and 16, with more bands of photometric data, i.e., spectroscopy and the SAGE photometry, UBVRI and ugriz photometry. For the metallicity, we also did not found obvious advantage of the fitting in Figures 15 and 16, than that of SAGE+spectrum method in Section 5.1.

6. Discussion

6.1. The Sample Selection and Results discussion

Discussion of the sample and results of different methods:

For our sample, we have selected only 17 star clusters of M33, the brightest ones ($V < 17.5$) in the galaxy, which are the most massive star clusters. Since the distance modulus $(m-M)_0 = 24.64 \pm 0.15$, the absolute magnitude of our sample star clusters are $M_0 < -7.1$, for which the mass $> 5.8 \times 10^4$. Thus we only focus on the massive star clusters and our sample is not effected by the selection effect significantly.

We have derived the ages and metallicities of our sample star clusters, with both ULySS (Koleva et al. 2009) models, including the Vazdekis et al. (2010) and PEGASE-HR SSP models and the BC03 (Bruzual & Charlot 2003) SSP models. It is noted that the ages derived from the ULySS models lack young star clusters which are $log\ t < 7$ yr in the BC03 models, as the lower limit of ages are 10^8 and 10^7 for Vazdekis et al. (2010) and PEGASE-HR SSP models, respectively. Thus the results of young star clusters $log\ t < 7$ yr can only be found in that of BC03 models in our work. However, for the BC03 models, it is also noted that the number of star clusters with age $log\ t < 7$ yr from models of Padova 1994 tracks are much more than that from the models of Padova 2000 tracks in either fitting method 2 (Spectrum +SAGE photometry) or fitting method 3 (Spectrum + all the photometry), which may be due to the spectral library is not updated to that of Girardi (2000), compared to Padova 2000 tracks. It is also noted that the number of star clusters with age $log\ t < 7$ yr are comparable for that of the fitting method 2 (Spectrum +SAGE photometry) and fitting method 3 (Spectrum + all the photometry). After comparing our fitting results with the literature, we found that adding more-band of photometric data besides of SAGE photometry in the blue wavelength coverage actually dose not improve the fitting results substantially except reducing the fitting errors to some extent.

6.2. The age-metallicity degeneracy

It is well-known that the age-metallicity degeneracy exists in the SED or spectrum fitting. In order to investigate this point, we have done a series of works for testing. Figure 17 is the Monte-Carlo simulations for the spectrum of one randomly selected star cluster if we add a series of errors around 5% (which is the Gaussian distribution) to the spectrum and fit the age and metallicity with the PEGASE-HR models (black crosses) and Vazdekis models (red crosses). Apparently, we can see the age-metallicity degeneracy, especially for the Vazdekis models. Similarly, in Figure 18 we have shown the relations between metallicity and ages for the spectrum of one randomly selected star cluster with the Padova 2000 evolutionary tracks and Chabrier (2003) IMF. We have done the χ^2_{min}-fit for all the ages provided in the models and fit the metallicity. The situations of full-spectrum, SAGE photometry+Spectrum (method 2) and all photometry+Spectrum (method 3) are all plotted

and shown. We identify a trend of the age-metallicity degeneracy, but it is not significant in all the three fitting methods. In fact, we have checked more star clusters, and the results are various for different sources. However, the age-metallicity relation for this star cluster is quite typical. In addition, we also have tried different evolutionary tracks and IMFs, and the results are similar, although the results are slightly different.

6.3. The UV-excess of our sample

We compare the *GALEX* FUV, NUV photometry with the SAGE u_{SC} together with cluster age in Figure 19. The *GALEX* photometry (Mudd & Stane 2015) was done for the point sources. All the magnitudes and colors have been dereddened adopting the extinction law of Cardelli et al. (1989).

As indicated in the top left panel of Figure 19, there is a correlation between $NUV - u_{SC}$ vs. cluster age from the left columns of Table 7, which are derived from the spectroscopy+SAGE photometry fitting, but for the BC03 models with Padova 2000 stellar evolutionary tracks, and Chabrier (2003) IMF. Usually young, massive (O/B) stars which are currently formed in the young clusters are sources for the emission of UV lights. $NUV - u_{SC}$ shows a dependence on age with a correlation coefficient of $r = 0.44$ (solid line in Figure 19). Five intermediate-age clusters above 400 Myr (black squares, ID: 245, 70, 94, 221 and 214) are located further away from the general correlation of the sample, by showing bluer color $NUV - u_{SC}$ less than 0.2 (defined as the "UV-excess" in our work). These five clusters (black squares in the top left panel of Figure 19) have u_{SC} close to young clusters. However, they only have NUV excess (top right and bottom left panels in Figure 19), and the $FUV - u_{SC}$ colors are normal (bottom right panel in Figure 19). As the cluster grows old, its massive stars evolved. So that $NUV - u_{SC}$ color of the cluster becomes redder, and u_{SC} magnitude grows fainter at the same time. Young massive stars are supposed to be absent in these five clusters. However, they deviate from the monotonic trend of $NUV - u_{SC}$ vs. u_{SC} (top right and bottom left panels in Figure 19). Excluding these five clusters, $NUV - u_{SC}$ dependence on cluster age is enhanced with a correlation coefficient of $r = 0.76$ (solid line in Figure 19).

Excess emission in UV color has been observed in old populations, e.g., discovered in early-type galaxies (Deharveng et al. 1976; O'connell et al. 1986); Galactic globular clusters: 47 Tuc (O'Connell et al. 1997), NGC 6388 and NGC 6441 (Rey et al. 2007); and old open clusters: NGC 6791 (Buzzoni et al. 2012). A similar phenomenon has been modeled via numerical N-body simulations of Pang et al. (2016), which reproduced UV-excess in the SED of star clusters up to 600 Myr. Observational and theoretical evidences show that low-mass, small-envelope, helium-burning stars in the blue horizontal branch (BHB),

whose effective temperature reaches above 35000 K, are promising candidates for producing UV excess in old populations (Ree et al. 2007; Rey et al. 2007; Buzzoni et al. 2012; Bekki 2012). The morphology of BHB depends on metallicity. BHB stars are bluer with lower metallicity (Yi et al. 1999; Yoon et al. 2006). Two intermediate-age clusters (ID: SM 70, 214) with NUV excess have almost the lowest metallicity ([Fe/H] = −1.51 and −1.46, see mean metallicity of Table 7 with Chabrier (2003) and Salpeter (1955) IMFs) among our samples, which is consistent with the theoretical prediction. At the same time, metallicity of three another intermediate-age clusters (ID: SM 245, 94 and 221) are median or higher ([Fe/H] = −0.30, −0.30 and −0.63, see mean metallicity of Table 7 with Chabrier (2003) and Salpeter (1955) IMFs). Including helium enrichment, a metal-rich cluster can also produce BHB (Rich et al. 1997; Chung et al. 2013; Bekki 2012). Besides the BHB scenario, Bekki (2012) simulations found that a cluster with multiple populations can generate UV-excess when the younger generation was helium enhanced from AGBs of the first generation. Note that the age and metallicity are degenerated in producing blue color. However, with our current data, we cannot justify either BHB or multiple population scenarios.

We found a positive gradient in the $NUV - u_{SC}$ vs. clusters' distance to the center of M33 in Figure 20. The slope is $k = 0.23$ and the correlation coefficient $r = 0.49$. This color gradient is consistent with the age distribution of clusters. Younger cluster are located in the inner part of M33 (cross symbols), with bluer $NUV - u_{SC}$ color, while older generations are redder and idle around the outskirt (squared symbols). This color gradient with the slope of $k = 0.23$ is also an age gradient, consistent with the upper left panel in Figure 19, implying an inside out formation history for M33 galaxy.

To discover more UV-excess among intermediate-age or old star clusters in the Local Group, the Chinese Space Station Station Telescope (CSST) will be an essential equipment in the future, providing NUV photometry (down to 255 nm) with 10 times higher spatial resolution $\sim 0.15''$ (Cao et al. 2018; Gong et al. 2019) than $GALEX$. Given only five intermediate-age clusters with UV-excess observed in our small samples, this number will be significantly increased after CSST 's NUV survey of the Local Group.

7. Summary and Conclusions

In our work, we compared different fitting methods for star clusters with the stellar population synthesis models based on spectroscopy and photometry (SED) data. We choose a sample of 17 star clusters in M33 which lack previous spectroscopic observations. The spectra of our sample star clusters were taken with the BFOSC low-resolution spectrograph on the NAOC Xinglong 2.16-m reflector.

In fact, we applied three different fitting methods: 1) full-spectrum fitting with ULySS (Koleva et al. 2009) including the Vazdekis et al. (2010) and PEGASE-HR SSP models and Bruzual & Charlot (2003) models; 2) spectroscopy + blue-bands SAGE u_{SC} and v_{SAGE} photometry with Bruzual & Charlot (2003) models; 3) spectroscopy + photometry of SAGE u_{SC} and v_{SAGE} bands, UBVRI-bands and ugriz-bands, with Bruzual & Charlot (2003) models. For all the methods, when using the Bruzual & Charlot (2003) models, the evolutionary tracks of Padova 1994 and Padova 2000 with the IMFs of Chabrier (2003) and Salpeter (1955) have been applied separately. The $\chi^2_{\rm min}$ technique has been applied for all the fittings.

We found that

1. The fitting results of models with Padova 2000 tracks, for which the updated stellar spectral library of Girardi (2000) is applied, are significantly better than those of the Padova 1994 track in all the fittings overall, especially for fitting method 2 (spectroscopy + blue-bands SAGE u_{SC} and v_{SAGE} photometry) and method 3 (spectroscopy + photometry of SAGE u_{SC} and v_{SAGE} bands, UBVRI-bands and ugriz-band);

2. Adding the blue-band photometry (such as SAGE u_{SC} and v_{SAGE} bands) to the spectroscopy fitting can improve the precision of the fitting results significantly, i.e. the errors have been reduced significantly. The median differences between our fitting results and the literature becomes much smaller, especially for the Padova 2000 tracks model, to $0.04-0.08$ dex for ages *log t*. Thus the method is an effective way to combine the spectroscopy and the SEDs. On one hand, the spectra can provide more information, not only the continuum, but also the absorption lines. The SAGE v_{SAGE} magnitude is sensitive to metallicity since its bandwidth contains the CaII K line at λ =3933.44 Å. On the other hand, the SED constructed with photometry from the blue bands, e.g., SAGE u_{SC} and v_{SAGE}, is a good complement to the spectroscopy. The fitting results are consistent with those of Beasley et al. (2015) and Fan et al. (2014) in both ages and metallicities, except for a few outliers. In general, our results agree well with previous determinations.

3. Adding photometry in more bands, such as the UBVRI and ugriz, did not substantially extend the wavelength coverage and thus can not provide more information than method 2. It is found that the median difference has not been reduced, but slightly larger for ages *log t* of the Padova 2000 track model, from $0.04-0.08$ to 0.12 dex. Thus the results cannot be improved significantly. However, we found the fitting errors become much smaller, which can be found from Figure 15 and 16.

It is discovered that five candidate star clusters exhibit UV-excess in FUV and NUV bands. The true magnitude of the UV-excess is expected to be stronger. The CSST, being the only space telescope equipped with the NUV band, will validate and discover more

UV-excess star clusters in the Local Group.

Further, as the LAMOST survey (Zhao et al. 2012; Cui et al. 2012) has provides more than ten million of stellar spectra already, it is the largest spectroscopic dataset in the world currently. In addition, the project is still ongoing and the number is increasing. Since the limiting magnitudes of u_{SC} and v_{SAGE} bands of SAGE survey could reach $\sim 17-18$ mag with an SNR of $\sim$50, it can perfectly match the LAMOST magnitude range with high SNR. Thus the SAGE survey could be quite useful and complementary for the spectrum fitting of LAMOST spectra. Moreover, it has been demonstrated that the blue bands are very crucial for distinguishing different stellar populations.

We thank the anonymous referee for his/her thorough review and helpful comments and suggestions, which significantly contributed to improving the manuscript. This study is supported by the National Natural Science Foundation of China (NSFC) under grant Nos. 11988101, 11890694, U1631102; Sino-German Center Project GZ 1284; National Key Research and Development Program of China grant Nos. 2019YFA0405502, 2016YFA0400804; and the Youth Innovation Promotion Association (YIPA), Chinese Academy of Sciences. X.Y.P. expresses gratitude for support from the Research Development Fund of Xi'an Jiaotong Liverpool University (RDF-18-02-32) and the financial support of two grants of National Natural Science Foundation of China, Nos. 11673032 and 11503015. We thank Prof. Richard de Grijs for useful discussion and Dr. James E. Wicker for professional language revision.

REFERENCES

Beasley, M. A., San Roman, I., Gallart, C., Sarajedini, A., Aparicio, A., 2015, MNRAS, 451, 3400

Bekki, K. 2012, ApJ, 747, 78

Bruzual A., G., & Charlot, S. 2003, MNRAS, 344, 1000

Buzzoni, A., Bertone, E., Carraro, G., et al. 2012, ApJ, 749, 35

Buzzoni, A., & González-Lópezlira, R. A. 2008, ApJ, 686, 1007

Cao, Y., Gong, Y., Meng, X.-M., et al. 2018, MNRAS, 480, 2178

Cardelli, J. A., Clayton, G. C., & Mathis, J. S., 1989, ApJ, 345, 245

Chabrier, G., 2003, PASP, 115, 763

Chung, C., Lee, S.-Y., Yoon, S.-J., et al. 2013, ApJ, 769, L3

Cui, X.-Q., Zhao, Y.-H., Chu, Y.-Q., et al., 2012, RAA, 12, 1197

Chandar, R., Bianchi, L., Ford, H. C., Sarajedini, A. 2002, ApJ, 564, 712

Chandar, R., Puzia, T. H., Sarajedini, A., Goudfrooij, P. 2006, ApJ, 646, L107

Chen, B. Q., Liu, X. W, et al., 2015, RAA, 15, 1392

Chen, B. Q., Liu, X. W., Xiang, M. S., et al. 2016, AJ, 152, 45

Deharveng, J. M., Laget, M., Monnet, G., et al. 1976, A&A, 50, 371

de Grijs, R., Fritze-v. Alvensleben, U., Anders, P., et al. 2003, MNRAS, 342, 259

Fan, Z., Ma, J., de Grijs, R., Yang, Y., & Zhou, X. 2006, MNRAS, 371, 1648

Fan, Z., Huang, Y. F., Li, J. Z., et al. 2011, RAA, 11, 1298

Fan, Z., Huang, Y. F., Li, J. Z., et al. 2012, RAA, 12, 829

Fan, Z., & de Grijs, R., 2014, ApJS, 211, 22

Fan, Z., de Grijs, R., Chen, B., et al. 2016, AJ, 152, 208

Fan, Zhou, Wang, Huijuan, Jiang, Xiaojun, et al., 2016, PASP, 128, 5005

Fan, Z. & Yang, Y.-B., 2014, in: Y. Meiron, S. Li, F.-K. Liu & R. Spurzem (eds.), *Proceedings IAU Symposium, Volume 10, Symposium S312 (Star Clusters and Black Holes in Galaxies across Cosmic Time)* August 2014 , pp. 201-202

Fan, Z., Zhao, G., Wang, W., et al. 2018, Progress in Astronomy, 36, 101

Galleti, S., Bellazzini, M., & Ferraro, F. R. 2004, A&A, 423, 925

Girardi, L., Bressan, A., Bertelli, G., & Chiosi, C. 2000, A&AS, 141, 371

Gong, Y., Liu, X., Cao, Y., et al. 2019, ApJ, 883, 203

Han, Z., Podsiadlowski, P., & Lynas-Gray, A.E. 2007, MNRAS, 380, 1098

Koleva, M., Prugniel, Ph., Bouchard, A., & Wu, Y. 2009, A&A, 501, 1269

Kotulla, R., Fritze, U., Weilbacher, P., & Anders, P., 2009, MNRAS, 396, 462

Le Borgne, D., Rocca-Volmerange, B., Prugniel, P., et al., 2004, A&A, 425, 881

Lilly, T., & Fritze-v. Alvensleben, U. 2006, A&A, 457, 467

Lilly, T., Fritze-v. Alvensleben, U., & de Grijs, R. 2009, Globular Clusters - Guides to Galaxies, Eso Astrophysics Symposia. ISBN 978-3-540-76960-6. Springer Berlin Heidelberg, 2009, p. 307

Ma, J., Yang, Y. B., Burstein, D., et al. 2007, ApJ, 659, 359

Ma, J., Fan, Z., de Grijs, R., et al. 2009, AJ, 137, 4884

Ma, J., Wang, S., Wu, Z., et al. 2011, AJ, 141, 86

Ma, J., Wang, S., Wu, Z., et al. 2012, AJ, 143, 29

Ma, J., 2013, AJ, 145, 88

Mackey, A. D., Ferguson, A. M. N., Huxor, A. P., et al. 2019, MNRAS, 484, 1756

Massey, P., Strobel, K., Barnes, J. V., & Anderson, E. 1988, ApJ, 328, 315

McConnachie, A. W., et al. 2009, Nature, 461, 66

Mudd, D. & Stanek, K. Z., 2015, MNRAS, 450, 3811

O'Connell, R. W., Dorman, B., Shah, R. Y., et al. 1997, AJ, 114, 1982

O'connell, R.W., Thuan, T.X., & Puschell, J.J. 1986, ApJ, 303, L37

Pang, X.-Y., Olczak, C., Guo, D.-F., et al. 2016, RAA, 16, 37

Prugniel, Ph. & Soubiran, C., 2001, A&A, 369, 1048

Prugniel, Ph., Soubiran, C., Koleva, M., Le Borgne, D. 2007, arXiv:astro-ph/0703658

Ree, C. H., Lee, Y.-W., Yi, S. K., et al. 2007, ApJS, 173, 607

Rey, S.-C., Rich, R. M., Sohn, S. T., et al. 2007, ApJS, 173, 643

Rich, R. M., Sosin, C., Djorgovski, S. G., et al. 1997, ApJ, 484, L25

Roser, S., Schilbach, E., Schwan, H., et al., 2008, A&A, 488, 401

Sakari, C. M. 2019, Star Clusters: From the Milky Way to the Early Universe Proceedings IAU Symposium No. 351, 2019, A. Bragaglia, M.B. Davies, A. Sills & E. Vesperini, eds., arXiv, 1907.1329

Salpeter, E. E. 1955, ApJ, 121, 161

Sánchez-Blázquez, P., Peletier, R. F.; Jiménez-Vicente, J., et al. 2006, MNRAS, 371, 703

San Roman, I., Sarajedini, A., Garnett, D. R., & Holtzman, J. A. 2009, ApJ, 699, 839

San Roman, I., Sarajedini, 1108 A., & Aparicio, A. 2010, ApJ, 720, 1674

Sarajedini, A., Geisler, D., Schommer, R., & Harding, P. 2000, AJ, 120, 2437

Sarajedini, A., & Mancone, C. L. 2007, AJ, 134, 447

Schommer, R. A., Christian, C. A., Caldwell, N., Bothun, G. D., Huchra, J. 1991, AJ, 101, 873

Sharina, M. E., Chandar, R., Puzia, T. H., Goudfrooij, P., Davoust, E. 2010, MNRAS, 405, 839

van der Marel, R. P., Fardal, M., Besla, G., et al. 2012, ApJ, 753, 8

van der Marel, R. P., Fardal, M. A., Sohn, S. T., et al., 2019, ApJ, 872, 24

Vazdekis A., 1999, ApJ, 513, 224

Vazdekis, A., Sánchez-Blázquez, P., Falcón-Barroso, J., et al. 2010, MNRAS, 404, 1639

Wang, S., Fan, Z., Ma, J., de Grijs, R., & Zhou, X. 2010, AJ, 139, 1438

Wang, S., Ma, J., Fan, Z., et al. 2012, AJ, 144, 191

Yi, S., Lee, Y.-W., Woo, J.-H., et al. 1999, ApJ, 513, 128

Yoon, S.-J., Yi, S. K., & Lee, Y.-W. 2006, Science, 311, 1129

Werle, A., Cid Fernandes, R., Vale Asari, N., et al. 2019, MNRAS, 483, 2382

Zhao, G., Zhao, Y.-H., Chu, Y.-Q, et al. 2012, RAA, 12, 723

Zheng, J., Zhao, G., Wang, W., Fan, Z., Tan, K., Li C., Zuo F. 2018, RAA, 18, 147

Zheng, J., Zhao, G., Wang, W., Fan, Z., Tan, K., Li C., Zuo F. 2019, RAA, 19, 3

Zheng, J., Zhao, G., Wang, W., Fan, Z., Zhao, J., Tan, K. 2019, Astronomical Research & Technology, 16, 93

This preprint was prepared with the AAS LaTeX macros v5.0.

Table 1. The observation informations of our sample star clusters in M33. The ID_{SM07}, RA, Dec and V-band magnitude are from the Table 3 of Sarajedini & Mancone (2007).

ID_{SM07}	R.A. (J2000)	Dec (J2000)	V-mag (mag)	Date (yyyy/mm/dd)	Expose Time (sec)
197	01:33:50.85	+30:38:34.5	16.39	2015/10/09	2400+1800
198	01:33:50.90	+30:38:55.5	16.76	2015/10/09	3600
284	01:34:03.12	+30:52:13.9	16.83	2015/10/09	3600
243	01:33:57.87	+30:33:25.7	17.00	2015/10/09	3600
245	01:33:58.01	+30:45:45.2	17.14	2015/10/10	3600
371	01:34:19.89	+30:36:12.7	17.16	2015/10/10	3600
140	01:33:37.24	+30:34:13.9	17.15	2015/10/11	3600
402	01:34:30.20	+30:38:13.0	17.19	2015/10/11	3600
427	01:34:43.70	+30:47:37.9	17.20	2015/10/11	3600
206	01:33:52.20	+30:29:03.8	17.29	2015/10/11	3600
70	01:33:23.10	+30:33:00.5	17.38	2015/10/19	3600
94	01:33:28.70	+30:36:37.5	17.38	2015/10/19	3600
228	01:33:56.18	+30:38:39.8	17.38	2015/10/19	3600
221	01:33:55.00	+30:32:14.5	17.42	2015/10/19	3600
85	01:33:26.75	+30:33:21.4	17.45	2015/10/19	3600
214	01:33:53.69	+30:48:21.5	17.45	2015/10/19	3600
329	01:34:10.09	+30:45:29.4	17.48	2015/10/19	3600

Table 2. The physical parameters, ages and metallicities of our sample star clusters derived from full-spectrum fits with Vazdekis model and PEGASE-HR models of ULySS.

ID	Vazdekis model			PEGASE-HR model		
	log t (yr)	[Fe/H] (dex)	χ^2_{min}/dof	log t (yr)	[Fe/H] (dex)	χ^2_{min}/dof
197	9.93 ± 0.07	-2.32 ± 0.01	0.13	10.02 ± 0.04	-2.13 ± 0.05	0.12
198	7.82 ± 0.01	-2.32 ± 0.01	0.36	7.17 ± 0.02	-0.67 ± 0.13	0.34
284	8.56 ± 0.01	0.22 ± 0.01	0.43	8.26 ± 0.03	0.24 ± 0.09	0.41
243	9.17 ± 0.02	-2.31 ± 0.07	2.27	10.03 ± 0.07	-2.18 ± 0.03	2.96
245	8.63 ± 0.05	-1.22 ± 0.08	2.46	8.81 ± 0.03	-2.30 ± 0.01	4.74
371	8.42 ± 0.02	-1.04 ± 0.05	0.38	7.82 ± 0.02	-0.18 ± 0.06	0.37
140	8.39 ± 0.02	-0.86 ± 0.05	0.08	7.84 ± 0.02	0.23 ± 0.05	0.08
402	10.05 ± 0.03	-1.50 ± 0.10	0.12	10.13 ± 0.03	-1.64 ± 0.06	0.11
427	8.56 ± 0.02	-0.16 ± 0.05	0.14	8.51 ± 0.04	0.03 ± 0.08	0.14
206	10.14 ± 0.05	-1.65 ± 0.06	0.59	9.91 ± 0.02	-2.30 ± 0.05	0.55
70	8.51 ± 0.01	-1.30 ± 0.09	0.90	7.90 ± 0.03	-0.38 ± 0.07	0.87
94	8.62 ± 0.01	0.22 ± 0.01	0.42	8.62 ± 0.02	0.22 ± 0.05	0.36
228	8.05 ± 0.02	-1.61 ± 0.15	0.64	7.52 ± 0.02	0.14 ± 0.04	0.65
221	9.13 ± 0.01	-1.71 ± 0.05	1.91	7.75 ± 0.02	0.46 ± 0.07	2.03
85	8.04 ± 0.01	-0.43 ± 0.12	0.13	7.75 ± 0.01	0.70 ± 0.01	0.13
214	7.86 ± 0.01	0.22 ± 0.01	0.74	7.78 ± 0.01	0.60 ± 0.04	0.74
329	8.16 ± 0.01	0.22 ± 0.01	2.07	7.92 ± 0.02	0.31 ± 0.06	2.06

Table 3. Same as in Table 2 but from full-spectrum fitting with Bruzual & Charlot (2003) models and Padova 1994 stellar evolutionary tracks. Both the Chabrier (2003) IMF and Salpeter (1955) IMF were adopted for the fitting separately.

ID	Chabrier (2003) IMF			Salpeter (1955) IMF		
	log t (yr)	[Fe/H] (dex)	χ^2_{min}/dof	log t (yr)	[Fe/H] (dex)	χ^2_{min}/dof
197	$6.720^{+0.179}_{0.000}$	$0.19^{+0.00}_{-0.00}$	0.31	$6.720^{+0.180}_{0.000}$	$0.19^{+0.00}_{-0.00}$	0.31
198	$6.820^{+0.156}_{-0.083}$	$0.56^{+0.00}_{-0.20}$	0.72	$6.820^{+0.155}_{-0.082}$	$0.56^{+0.00}_{-0.20}$	0.72
284	$8.357^{+1.072}_{-1.449}$	$-1.27^{+0.00}_{-0.00}$	0.45	$8.357^{+1.053}_{-1.448}$	$-1.27^{+0.00}_{-0.00}$	0.45
243	$6.980^{+2.186}_{-0.331}$	$0.37^{+0.00}_{-1.91}$	0.69	$6.980^{+2.185}_{-0.330}$	$0.37^{+0.00}_{-1.92}$	0.69
245	$6.920^{+2.260}_{-0.246}$	$0.28^{+0.00}_{-1.69}$	1.00	$6.920^{+2.259}_{-0.245}$	$0.28^{+0.00}_{-1.69}$	1.00
371	$8.057^{+0.890}_{-1.361}$	$-0.19^{+0.00}_{-0.00}$	0.37	$8.057^{+0.885}_{-1.360}$	$-0.19^{+0.00}_{-0.00}$	0.38
140	$6.660^{+0.051}_{-0.165}$	$-2.01^{+0.38}_{-0.00}$	0.31	$6.600^{+0.106}_{-0.103}$	$-1.92^{+0.42}_{-0.00}$	0.32
402	$10.106^{+0.000}_{-1.134}$	$-1.59^{+1.69}_{-0.00}$	0.38	$10.011^{+0.000}_{-1.029}$	$-1.69^{+1.79}_{-0.00}$	0.37
427	$9.057^{+0.000}_{-1.036}$	$-1.31^{+0.00}_{-0.00}$	0.40	$9.057^{+0.000}_{-1.033}$	$-1.36^{+0.00}_{-0.00}$	0.41
206	$10.097^{+0.000}_{-1.207}$	$-1.13^{+1.67}_{-0.00}$	0.76	$10.097^{+0.000}_{-1.197}$	$-1.27^{+1.77}_{-0.00}$	0.76
70	$9.007^{+0.000}_{-1.609}$	$-1.45^{+0.00}_{-0.00}$	0.98	$9.007^{+0.000}_{-1.573}$	$-1.50^{+0.00}_{-0.00}$	0.98
94	$8.707^{+0.819}_{-1.555}$	$-1.78^{+0.00}_{-0.00}$	0.70	$8.707^{+0.789}_{-1.542}$	$-1.83^{+0.00}_{-0.00}$	0.70
228	$6.940^{+2.368}_{-0.186}$	$-0.00^{+0.00}_{-1.28}$	0.56	$6.940^{+2.361}_{-0.185}$	$-0.00^{+0.00}_{-1.27}$	0.56
221	$8.907^{+0.000}_{-1.779}$	$-1.92^{+0.00}_{-0.00}$	1.83	$8.907^{+0.000}_{-1.768}$	$-1.97^{+0.00}_{-0.00}$	1.83
85	$8.707^{+0.651}_{-1.379}$	$-1.87^{+0.00}_{-0.00}$	0.29	$8.707^{+0.591}_{-1.349}$	$-1.92^{+0.00}_{-0.00}$	0.30
214	$8.907^{+0.000}_{-1.534}$	$-1.64^{+0.00}_{-0.00}$	0.60	$8.907^{+1.313}_{-1.500}$	$-1.69^{+0.00}_{-0.00}$	0.60
329	$9.007^{+0.000}_{-1.659}$	$-2.25^{+0.00}_{-0.00}$	1.11	$8.957^{+0.000}_{-1.618}$	$-2.25^{+0.00}_{-0.00}$	1.12

Table 4. Same as in Table 3 but from full-spectrum fitting with Padova 2000 stellar evolutionary tracks of the Bruzual & Charlot (2003) models. Both theChabrier (2003) IMF and Salpeter (1955) IMF were adopted for the fitting separately.

ID	Chabrier (2003) IMF			Salpeter (1955) IMF		
	log t (yr)	[Fe/H] (dex)	χ^2_{min}/dof	log t (yr)	[Fe/H] (dex)	χ^2_{min}/dof
197	$6.900^{+1.156}_{0.000}$	$-1.00^{+0.00}_{-0.00}$	0.32	$6.900^{+1.157}_{0.000}$	$-1.00^{+0.00}_{-0.00}$	0.32
198	$6.940^{+0.657}_{-0.046}$	$0.16^{+0.00}_{-0.35}$	1.19	$6.940^{+0.656}_{-0.045}$	$0.16^{+0.00}_{-0.35}$	1.24
284	$8.307^{+1.171}_{-1.192}$	$-1.26^{+0.00}_{-0.00}$	0.45	$8.307^{+1.082}_{-1.193}$	$-1.26^{+0.00}_{-0.00}$	0.45
243	$6.980^{+2.354}_{-0.277}$	$0.06^{+0.00}_{-1.25}$	0.80	$6.960^{+2.196}_{-0.255}$	$0.26^{+0.00}_{-1.43}$	0.79
245	$6.980^{+2.279}_{-0.270}$	$0.06^{+0.00}_{-1.24}$	1.03	$6.960^{+2.310}_{-0.249}$	$0.03^{+0.00}_{-1.19}$	1.03
371	$8.057^{+0.958}_{-1.375}$	$-0.16^{+0.00}_{-0.00}$	0.37	$6.800^{+2.253}_{-0.214}$	$-0.42^{+0.00}_{-0.47}$	0.37
140	$7.544^{+1.584}_{-0.686}$	$-0.71^{+0.00}_{-0.00}$	0.35	$7.544^{+1.582}_{-0.684}$	$-0.71^{+0.00}_{-0.00}$	0.35
402	$10.097^{+0.000}_{-1.082}$	$-1.49^{+1.60}_{-0.00}$	0.37	$10.000^{+0.000}_{-0.995}$	$-1.58^{+1.75}_{-0.00}$	0.37
427	$9.107^{+0.000}_{-1.102}$	$-1.26^{+0.00}_{-0.00}$	0.40	$9.107^{+0.000}_{-1.094}$	$-1.32^{+0.00}_{-0.00}$	0.41
206	$9.989^{+0.000}_{-0.988}$	$-1.07^{+0.00}_{-0.00}$	0.74	$9.989^{+0.000}_{-0.983}$	$-1.16^{+0.00}_{-0.00}$	0.74
70	$9.057^{+0.000}_{-1.480}$	$-1.26^{+0.00}_{-0.00}$	0.94	$9.057^{+0.000}_{-1.481}$	$-1.26^{+0.00}_{-0.00}$	0.95
94	$8.657^{+0.710}_{-1.528}$	$-1.45^{+0.00}_{-0.00}$	0.71	$8.607^{+0.704}_{-1.483}$	$-1.36^{+0.00}_{-0.00}$	0.72
228	$6.940^{+2.402}_{-0.193}$	$-0.03^{+0.00}_{-0.99}$	0.56	$6.940^{+2.396}_{-0.193}$	$-0.03^{+0.00}_{-0.99}$	0.56
221	$8.857^{+0.000}_{-1.796}$	$-1.65^{+0.00}_{-0.00}$	1.83	$8.857^{+0.000}_{-1.797}$	$-1.65^{+0.00}_{-0.00}$	1.83
85	$8.557^{+0.695}_{-1.408}$	$-1.42^{+0.00}_{-0.00}$	0.31	$8.507^{+0.729}_{-1.360}$	$-1.39^{+0.00}_{-0.00}$	0.31
214	$8.957^{+1.299}_{-1.514}$	$-1.49^{+0.00}_{-0.00}$	0.60	$8.907^{+1.096}_{-1.456}$	$-1.42^{+0.00}_{-0.00}$	0.60
329	$8.607^{+1.345}_{-2.172}$	$-0.74^{+0.00}_{-0.00}$	1.10	$8.557^{+1.275}_{-2.121}$	$-0.68^{+0.00}_{-0.00}$	1.10

Table 5. The photometry of our sample star clusters. The SM IDs are from Sarajedini & Mancone (2007). The $u_{\rm SC}$ and $v_{\rm SAGE}$ are from the SAGE survey. The aperture correction have been done and calibrated in the AB system.

ID	$u_{\rm SC}$ (mag)	$v_{\rm SAGE}$ (mag)
197	16.17 ± 0.01	16.33 ± 0.01
198	17.00 ± 0.03	17.06 ± 0.03
284	18.30 ± 0.02	17.49 ± 0.03
243	17.29 ± 0.01	17.31 ± 0.02
245	18.25 ± 0.02	17.76 ± 0.03
371	17.83 ± 0.01	17.39 ± 0.03
140	18.06 ± 0.02	17.55 ± 0.02
402	18.76 ± 0.03	18.27 ± 0.05
427	18.95 ± 0.04	18.19 ± 0.05
206	19.46 ± 0.04	19.07 ± 0.07
70	18.51 ± 0.02	18.11 ± 0.03
94	19.03 ± 0.04	18.33 ± 0.04
228	18.54 ± 0.03	18.36 ± 0.05
221	19.69 ± 0.07	19.56 ± 0.13
85	18.19 ± 0.02	17.83 ± 0.03
214	18.57 ± 0.02	18.08 ± 0.04
329	19.23 ± 0.05	18.30 ± 0.05

Table 6. Same as in Table 3 but from the spectroscopy+ SAGE photometry fitting. BC03 models with Padova 1994 stellar evolutionary tracks, and the Chabrier (2003) IMF and Salpeter (1955) IMF were adopted.

ID	Chabrier (2003) IMF			Salpeter (1955) IMF		
	log t (yr)	[Fe/H] (dex)	χ^2_{min}/dof	log t (yr)	[Fe/H] (dex)	χ^2_{min}/dof
197	$6.660^{+0.077}_{-0.184}$	$-1.59^{+0.00}_{-0.27}$	0.56	$6.660^{+0.078}_{-0.184}$	$-1.59^{+0.00}_{-0.27}$	0.56
198	$6.820^{+0.103}_{-0.064}$	$0.56^{+0.00}_{-0.14}$	1.57	$6.820^{+0.102}_{-0.063}$	$0.56^{+0.00}_{-0.14}$	1.62
284	$8.657^{+0.403}_{-0.563}$	$-0.56^{+0.00}_{-1.67}$	0.80	$8.657^{+0.402}_{-0.563}$	$-0.56^{+0.00}_{-0.00}$	0.81
243	$6.980^{+0.967}_{-0.241}$	$0.19^{+0.36}_{-1.52}$	0.84	$6.980^{+0.967}_{-0.240}$	$0.19^{+0.37}_{-1.52}$	0.85
245	$6.580^{+0.111}_{-0.081}$	$-2.25^{+0.34}_{-0.00}$	1.59	$6.580^{+0.110}_{-0.081}$	$-2.25^{+0.33}_{-0.00}$	1.59
371	$8.157^{+0.865}_{-0.309}$	$-2.25^{+0.00}_{-0.00}$	0.55	$8.157^{+0.861}_{-0.315}$	$-2.25^{+0.00}_{-0.00}$	0.55
140	$6.540^{+0.158}_{-0.042}$	$-2.25^{+0.29}_{-0.00}$	0.46	$6.560^{+0.131}_{-0.061}$	$-2.20^{+0.29}_{-0.00}$	0.47
402	$9.942^{+0.000}_{-0.848}$	$-1.55^{+0.98}_{-0.00}$	0.51	$9.903^{+0.000}_{-0.805}$	$-1.59^{+1.01}_{-0.00}$	0.51
427	$9.007^{+0.362}_{-0.561}$	$-0.47^{+0.78}_{-1.56}$	0.53	$9.007^{+0.382}_{-0.571}$	$-0.52^{+0.83}_{-1.55}$	0.53
206	$9.107^{+0.539}_{-0.302}$	$0.47^{+0.00}_{-1.38}$	0.91	$9.057^{+0.452}_{-0.285}$	$0.56^{+0.00}_{-0.92}$	0.92
70	$6.640^{+0.056}_{-0.141}$	$-2.25^{+0.29}_{-0.00}$	1.06	$6.600^{+0.085}_{-0.100}$	$-2.16^{+0.28}_{-0.00}$	1.06
94	$8.907^{+0.538}_{-0.857}$	$-1.78^{+1.57}_{-0.00}$	1.03	$8.857^{+0.421}_{-0.818}$	$-1.69^{+1.63}_{-0.00}$	1.05
228	$6.640^{+0.061}_{-0.142}$	$-2.01^{+0.29}_{-0.00}$	0.61	$6.620^{+0.075}_{-0.121}$	$-1.97^{+0.38}_{-0.00}$	0.61
221	$6.580^{+0.124}_{-0.084}$	$-2.25^{+0.51}_{-0.00}$	2.03	$6.580^{+0.124}_{-0.084}$	$-2.25^{+0.50}_{-0.00}$	2.03
85	$6.820^{+0.159}_{-0.056}$	$-0.38^{+0.38}_{-0.25}$	0.39	$6.820^{+0.156}_{-0.057}$	$-0.33^{+0.33}_{-0.29}$	0.41
214	$6.580^{+0.109}_{-0.081}$	$-2.20^{+0.32}_{-0.00}$	0.68	$6.580^{+0.108}_{-0.081}$	$-2.20^{+0.31}_{-0.00}$	0.68
329	$8.657^{+0.399}_{-0.616}$	$-0.19^{+0.00}_{-0.00}$	1.22	$8.657^{+0.398}_{-0.615}$	$-0.19^{+0.00}_{-0.00}$	1.22

Table 7. Same as in Table 6 from spectroscopy+ SAGE photometry fitting, but for the BC03 models with Padova 2000 stellar evolutionary tracks. The Chabrier (2003) IMF and Salpeter (1955) IMF were adopted separately.

ID	Chabrier (2003) IMF			Salpeter (1955) IMF		
	log t (yr)	[Fe/H] (dex)	χ^2_{min}/dof	log t (yr)	[Fe/H] (dex)	χ^2_{min}/dof
197	$6.740^{+0.053}_{-0.230}$	$-0.29^{+0.00}_{-0.00}$	0.38	$6.680^{+0.819}_{-0.207}$	$-1.23^{+0.00}_{-0.00}$	0.53
198	$6.940^{+0.564}_{-0.037}$	$0.13^{+0.00}_{-0.32}$	1.63	$6.940^{+0.649}_{-0.035}$	$0.13^{+0.00}_{-0.33}$	1.82
284	$8.657^{+0.235}_{-1.362}$	$0.26^{+0.00}_{-0.00}$	0.65	$8.707^{+0.399}_{-0.582}$	$-0.55^{+0.00}_{-0.00}$	0.80
243	$7.000^{+1.774}_{-0.256}$	$0.16^{+0.00}_{-1.23}$	0.85	$6.980^{+0.943}_{-0.231}$	$0.16^{+0.00}_{-1.20}$	0.86
245	$8.757^{+0.329}_{-1.579}$	$-0.20^{+0.00}_{-0.00}$	1.43	$8.357^{+0.627}_{-0.598}$	$-0.39^{+0.00}_{-0.00}$	1.93
371	$6.800^{+2.126}_{-0.060}$	$-0.39^{+0.00}_{-0.29}$	0.39	$7.857^{+0.584}_{-0.877}$	$0.03^{+0.00}_{-0.00}$	0.52
140	$8.657^{+0.457}_{-1.370}$	$-0.78^{+0.00}_{-0.00}$	0.45	$8.307^{+0.768}_{-0.640}$	$-1.23^{+0.00}_{-0.00}$	0.80
402	$9.989^{+0.000}_{-0.889}$	$-1.32^{+1.13}_{-0.00}$	0.38	$9.929^{+0.000}_{-0.774}$	$-1.61^{+1.08}_{-0.00}$	0.50
427	$9.007^{+0.333}_{-0.480}$	$-0.23^{+0.00}_{-0.00}$	0.46	$9.007^{+0.137}_{-0.440}$	$-0.29^{+0.00}_{-0.00}$	0.48
206	$9.157^{+1.109}_{-0.291}$	$0.29^{+0.00}_{-1.25}$	0.80	$9.157^{+0.709}_{-0.268}$	$0.26^{+0.00}_{-1.14}$	0.87
70	$9.057^{+0.694}_{-1.044}$	$-1.36^{+1.36}_{-0.00}$	0.95	$8.957^{+0.388}_{-0.935}$	$-1.65^{+1.18}_{-0.00}$	2.03
94	$8.607^{+0.279}_{-1.717}$	$0.22^{+0.00}_{-0.00}$	0.89	$8.607^{+0.504}_{-0.833}$	$-0.81^{+0.00}_{-0.00}$	0.96
228	$6.940^{+2.058}_{-0.179}$	$-0.03^{+0.00}_{-0.91}$	0.67	$7.220^{+1.059}_{-0.366}$	$0.13^{+0.00}_{-0.59}$	0.73
221	$8.707^{+0.467}_{-1.971}$	$0.26^{+0.00}_{-0.00}$	1.94	$8.907^{+0.969}_{-1.301}$	$-1.52^{+0.00}_{-0.00}$	2.14
85	$8.557^{+0.554}_{-1.202}$	$-1.16^{+0.00}_{-0.00}$	0.31	$6.820^{+0.157}_{-0.056}$	$-0.36^{+0.33}_{-0.27}$	0.40
214	$8.957^{+0.606}_{-1.279}$	$-1.26^{+1.40}_{-0.00}$	0.61	$8.907^{+0.408}_{-0.883}$	$-1.65^{+1.31}_{-0.00}$	1.20
329	$8.657^{+0.339}_{-1.795}$	$0.26^{+0.00}_{-0.00}$	1.14	$8.607^{+0.307}_{-0.575}$	$0.29^{+0.00}_{-0.00}$	1.20

Table 8. The photometry of our sample star clusters from references. The $UBVRI$ photometry are from Ma (2013), which are in the Johnson-Cousins system. The $ugriz$ photometry are from San Roman et al. (2010) which are in the AB system.

ID	U (mag)	B (mag)	V (mag)	R (mag)	I (mag)	u (mag)	g (mag)	r (mag)	i (mag)	z (mag)
197	15.54	16.41	16.38	16.51	16.60	99.99	99.99	99.99	99.99	99.99
198	16.37	17.09	16.78	16.38	15.65	16.81	16.81	16.63	16.24	15.77
284	17.04	17.17	16.82	16.66	16.39	99.99	99.99	99.99	99.99	99.99
243	16.52	17.20	17.08	16.97	16.72	17.07	17.10	17.20	17.15	17.05
245	17.24	17.50	17.17	16.94	16.64	17.90	17.31	17.26	17.14	16.98
371	17.04	17.39	17.12	16.98	16.76	17.72	17.22	17.22	17.20	17.08
140	17.12	17.42	17.12	16.94	16.68	17.38	17.09	17.05	16.95	16.82
402	17.85	17.88	17.13	16.62	16.11	18.62	17.57	17.06	16.72	16.44
427	17.78	17.75	17.25	16.97	16.58	99.99	99.99	99.99	99.99	99.99
206	18.30	18.13	17.29	16.77	16.28	18.83	17.78	17.18	16.82	16.59
70	17.56	17.89	17.59	17.41	17.09	18.01	17.63	17.65	17.55	17.47
94	17.92	18.05	17.71	17.50	17.20	18.45	17.89	17.85	17.70	17.58
228	17.93	18.47	18.17	17.90	17.34	18.32	18.18	18.07	17.72	17.30
221	18.87	18.94	18.59	18.44	18.25	99.99	99.99	99.99	99.99	99.99
85	17.39	17.84	17.57	17.40	17.11	17.79	17.49	17.50	17.39	17.31
214	17.56	17.89	17.55	17.34	17.00	18.23	17.69	17.63	17.50	17.34
329	17.81	17.90	17.48	17.34	16.94	18.70	17.95	18.00	17.98	17.90

Table 9. Same as in Table 6 but from the spectroscopy+ SAGE, UVBRI, ugriz photometry fitting. BC03 models with Padova 1994 stellar evolutionary tracks, and the Chabrier (2003) IMF and Salpeter (1955) IMF have been adopted separately for the fitting.

ID	Chabrier (2003) IMF			Salpeter (1955) IMF		
	log t (yr)	[Fe/H] (dex)	χ^2_{min}/dof	log t (yr)	[Fe/H] (dex)	χ^2_{min}/dof
197	$6.700^{+0.043}_{-0.072}$	$-0.14^{+0.57}_{-1.74}$	1.19	$6.700^{+0.044}_{-0.075}$	$-0.14^{+0.58}_{-1.75}$	1.19
198	$6.940^{+0.146}_{-0.017}$	$0.19^{+0.24}_{-0.19}$	3.17	$6.940^{+0.146}_{-0.017}$	$0.19^{+0.24}_{-0.19}$	3.38
284	$8.307^{+0.278}_{-0.356}$	$-0.42^{+0.00}_{-1.75}$	2.12	$8.307^{+0.276}_{-0.356}$	$-0.42^{+0.00}_{-1.77}$	2.13
243	$6.860^{+0.061}_{-0.110}$	$0.04^{+0.32}_{-0.25}$	1.81	$6.980^{+0.443}_{-0.109}$	$-0.24^{+0.25}_{-1.11}$	1.82
245	$6.520^{+0.065}_{-0.021}$	$-2.25^{+0.19}_{-0.00}$	2.09	$6.540^{+0.142}_{-0.040}$	$-2.20^{+0.19}_{-0.00}$	2.07
371	$7.740^{+0.305}_{-0.346}$	$-1.13^{+0.00}_{-0.57}$	0.86	$7.740^{+0.305}_{-0.345}$	$-1.13^{+0.00}_{-0.58}$	0.86
140	$7.602^{+0.526}_{-0.208}$	$-0.94^{+1.38}_{-0.45}$	2.73	$7.602^{+0.524}_{-0.210}$	$-0.89^{+1.33}_{-0.50}$	2.74
402	$9.916^{+0.000}_{-0.690}$	$-1.73^{+0.71}_{-0.00}$	0.87	$9.889^{+0.000}_{-0.661}$	$-1.83^{+0.76}_{-0.00}$	0.86
427	$9.057^{+0.465}_{-0.403}$	$-1.55^{+0.84}_{-0.00}$	1.64	$9.057^{+0.409}_{-0.389}$	$-1.59^{+0.87}_{-0.00}$	1.67
206	$10.000^{+0.000}_{-0.619}$	$-1.13^{+0.52}_{-0.88}$	1.57	$9.954^{+0.000}_{-0.598}$	$-1.17^{+0.55}_{-0.95}$	1.62
70	$6.820^{+0.094}_{-0.036}$	$-0.33^{+0.19}_{-0.18}$	2.52	$6.580^{+0.084}_{-0.065}$	$-2.01^{+0.18}_{-0.15}$	2.57
94	$6.520^{+0.074}_{-0.021}$	$-2.25^{+0.16}_{-0.00}$	2.08	$6.540^{+0.141}_{-0.040}$	$-2.25^{+0.21}_{-0.00}$	2.11
228	$7.240^{+0.432}_{-0.323}$	$0.19^{+0.23}_{-0.25}$	2.41	$7.240^{+0.433}_{-0.323}$	$0.19^{+0.23}_{-0.25}$	2.51
221	$8.207^{+0.340}_{-0.450}$	$-0.28^{+0.00}_{-0.00}$	2.38	$8.207^{+0.339}_{-0.449}$	$-0.28^{+0.00}_{-0.00}$	2.38
85	$6.840^{+0.122}_{-0.066}$	$-0.33^{+0.27}_{-0.23}$	1.55	$6.840^{+0.121}_{-0.065}$	$-0.33^{+0.27}_{-0.23}$	1.56
214	$6.580^{+0.082}_{-0.063}$	$-2.06^{+0.17}_{-0.17}$	1.34	$6.580^{+0.080}_{-0.061}$	$-2.06^{+0.16}_{-0.19}$	1.33
329	$6.540^{+0.125}_{-0.040}$	$-2.25^{+0.18}_{-0.00}$	7.28	$8.257^{+0.390}_{-0.369}$	$-1.13^{+0.00}_{-0.00}$	7.31

Table 10. Same as in Table 9 from the spectroscopy+ SAGE, UVBRI, ugriz photometry fitting, but for the Padova 2000 stellar evolutionary tracks. The Chabrier (2003) IMF and Salpeter (1955) IMF were adopted separately for the fitting.

ID	Chabrier (2003) IMF			Salpeter (1955) IMF		
	log t (yr)	[Fe/H] (dex)	χ^2_{min}/dof	log t (yr)	[Fe/H] (dex)	χ^2_{min}/dof
197	$6.560^{+0.193}_{-0.100}$	$-0.49^{+0.16}_{-0.18}$	1.20	$6.560^{+0.193}_{-0.100}$	$-0.49^{+0.16}_{-0.19}$	1.20
198	$6.940^{+0.132}_{-0.016}$	$0.13^{+0.00}_{-0.18}$	3.34	$6.940^{+0.132}_{-0.016}$	$0.13^{+0.00}_{-0.18}$	3.55
284	$8.307^{+0.294}_{-0.338}$	$-0.36^{+0.00}_{-0.00}$	2.05	$8.307^{+0.292}_{-0.338}$	$-0.36^{+0.00}_{-0.00}$	2.06
243	$6.860^{+0.060}_{-0.115}$	$-0.00^{+0.00}_{-0.22}$	1.79	$6.860^{+0.062}_{-0.114}$	$-0.00^{+0.00}_{-0.23}$	1.79
245	$8.007^{+0.280}_{-0.418}$	$0.13^{+0.00}_{-1.68}$	2.45	$8.007^{+0.281}_{-0.417}$	$0.13^{+0.00}_{-1.69}$	2.46
371	$7.757^{+0.336}_{-0.266}$	$-0.00^{+0.00}_{-1.62}$	0.77	$7.757^{+0.336}_{-0.268}$	$-0.00^{+0.00}_{-1.63}$	0.77
140	$7.591^{+0.526}_{-0.198}$	$-0.74^{+0.00}_{-0.37}$	2.73	$7.591^{+0.526}_{-0.196}$	$-0.74^{+0.00}_{-0.37}$	2.73
402	$9.889^{+0.000}_{-0.654}$	$-1.65^{+0.73}_{-0.00}$	0.83	$9.829^{+0.000}_{-0.608}$	$-1.65^{+0.74}_{-0.00}$	0.84
427	$9.057^{+0.489}_{-0.449}$	$-1.49^{+1.10}_{-0.00}$	1.74	$9.057^{+0.458}_{-0.424}$	$-1.55^{+1.16}_{-0.00}$	1.75
206	$9.989^{+0.000}_{-0.664}$	$-1.03^{+0.51}_{-0.00}$	1.52	$9.978^{+0.000}_{-0.655}$	$-1.10^{+0.54}_{-0.00}$	1.57
70	$6.820^{+0.094}_{-0.036}$	$-0.32^{+0.17}_{-0.19}$	2.53	$6.820^{+0.092}_{-0.035}$	$-0.32^{+0.17}_{-0.18}$	2.63
94	$8.157^{+0.285}_{-0.364}$	$-0.29^{+0.00}_{-0.00}$	2.36	$8.157^{+0.284}_{-0.362}$	$-0.29^{+0.00}_{-0.00}$	2.37
228	$7.240^{+0.336}_{-0.325}$	$0.13^{+0.00}_{-0.22}$	2.40	$7.240^{+0.335}_{-0.324}$	$0.13^{+0.00}_{-0.22}$	2.49
221	$8.207^{+0.388}_{-0.465}$	$-0.32^{+0.00}_{-0.00}$	2.36	$8.207^{+0.386}_{-0.463}$	$-0.32^{+0.00}_{-0.00}$	2.36
85	$6.840^{+0.122}_{-0.066}$	$-0.29^{+0.22}_{-0.27}$	1.54	$6.820^{+0.141}_{-0.045}$	$-0.26^{+0.18}_{-0.30}$	1.54
214	$7.628^{+0.641}_{-0.195}$	$-0.71^{+0.45}_{-0.38}$	1.75	$7.628^{+0.644}_{-0.194}$	$-0.71^{+0.45}_{-0.38}$	1.79
329	$8.157^{+0.591}_{-0.383}$	$-1.20^{+0.00}_{-0.00}$	7.24	$8.157^{+0.578}_{-0.381}$	$-1.20^{+0.00}_{-0.00}$	7.26

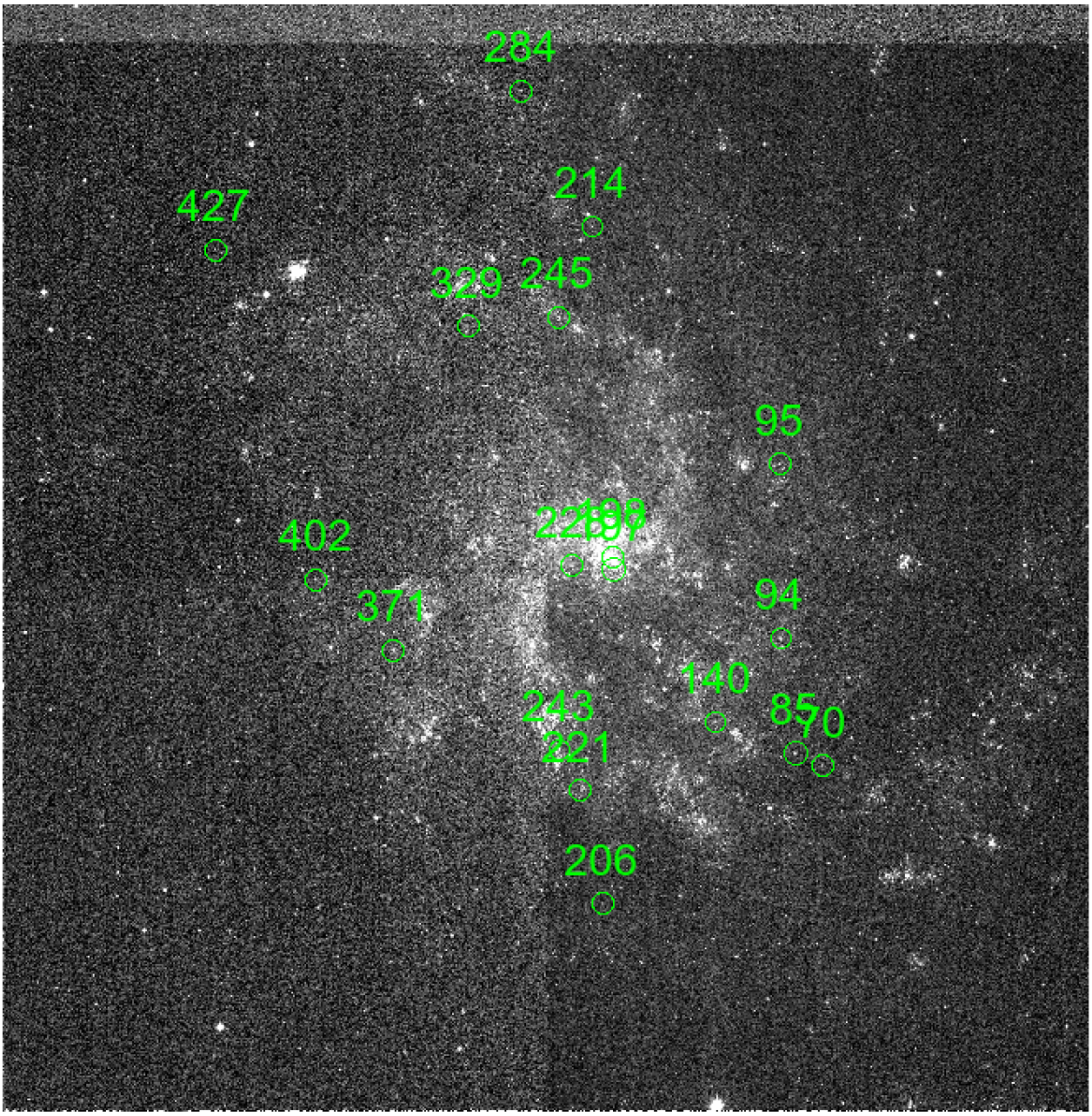


Fig. 1.— The spatial distribution of our M33 star cluster sample.

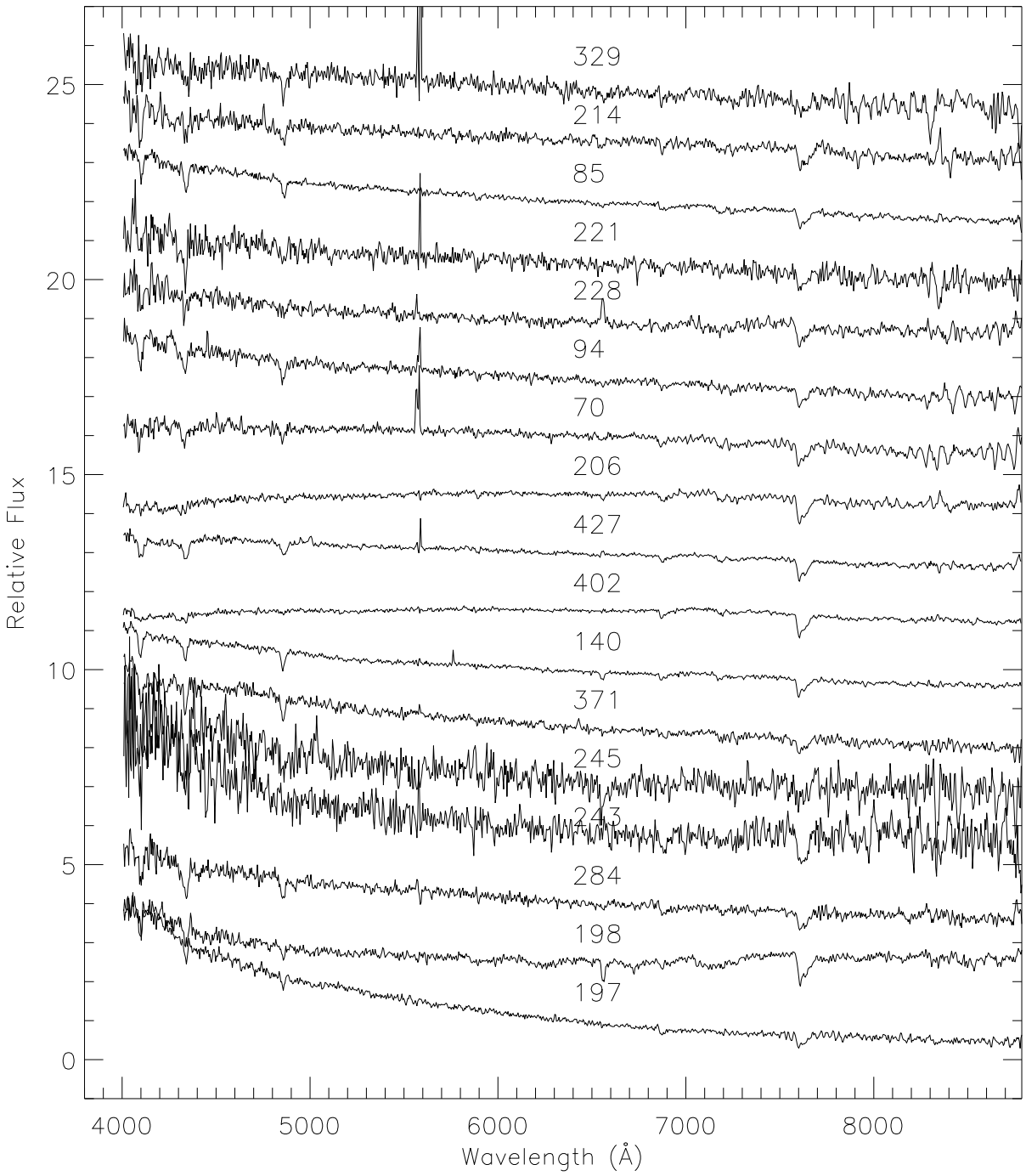


Fig. 2.— The normalized observed spectra of our star cluster sample in M31, which were taken from the 2.16-m telescope in Xinglong Observatory, NAOC.

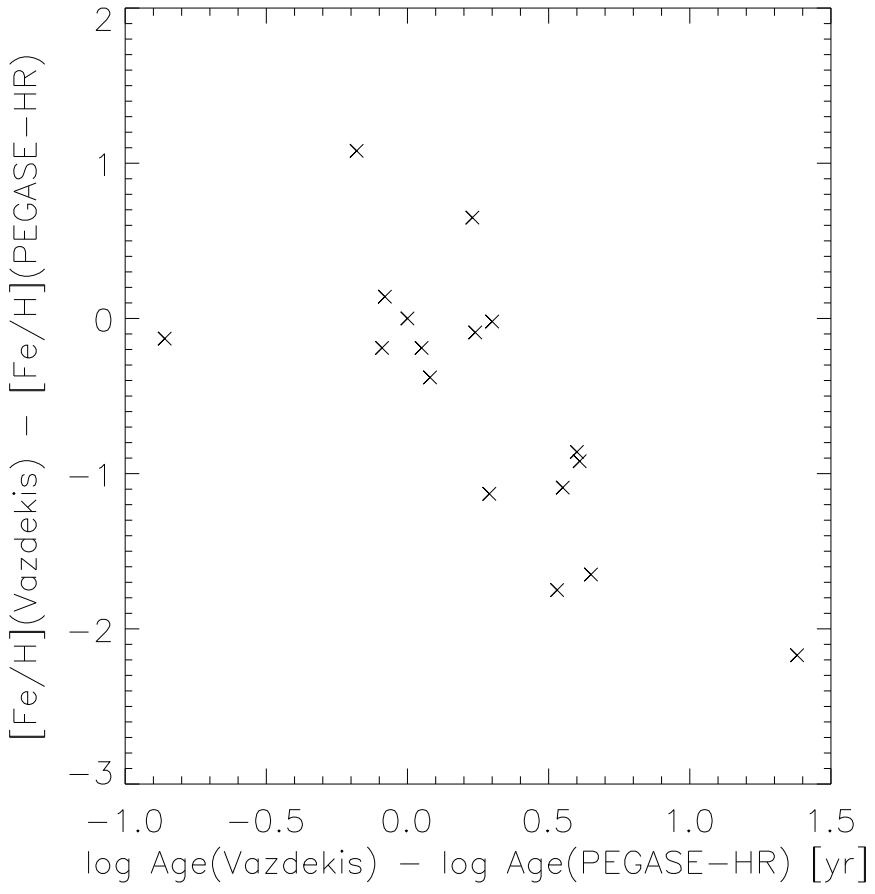


Fig. 3.— Self-comparisons of full-spectrum fitting results of Table 2, ages and metallicities derived with the Vazdekis models and PEGASE-HR models, respectively.

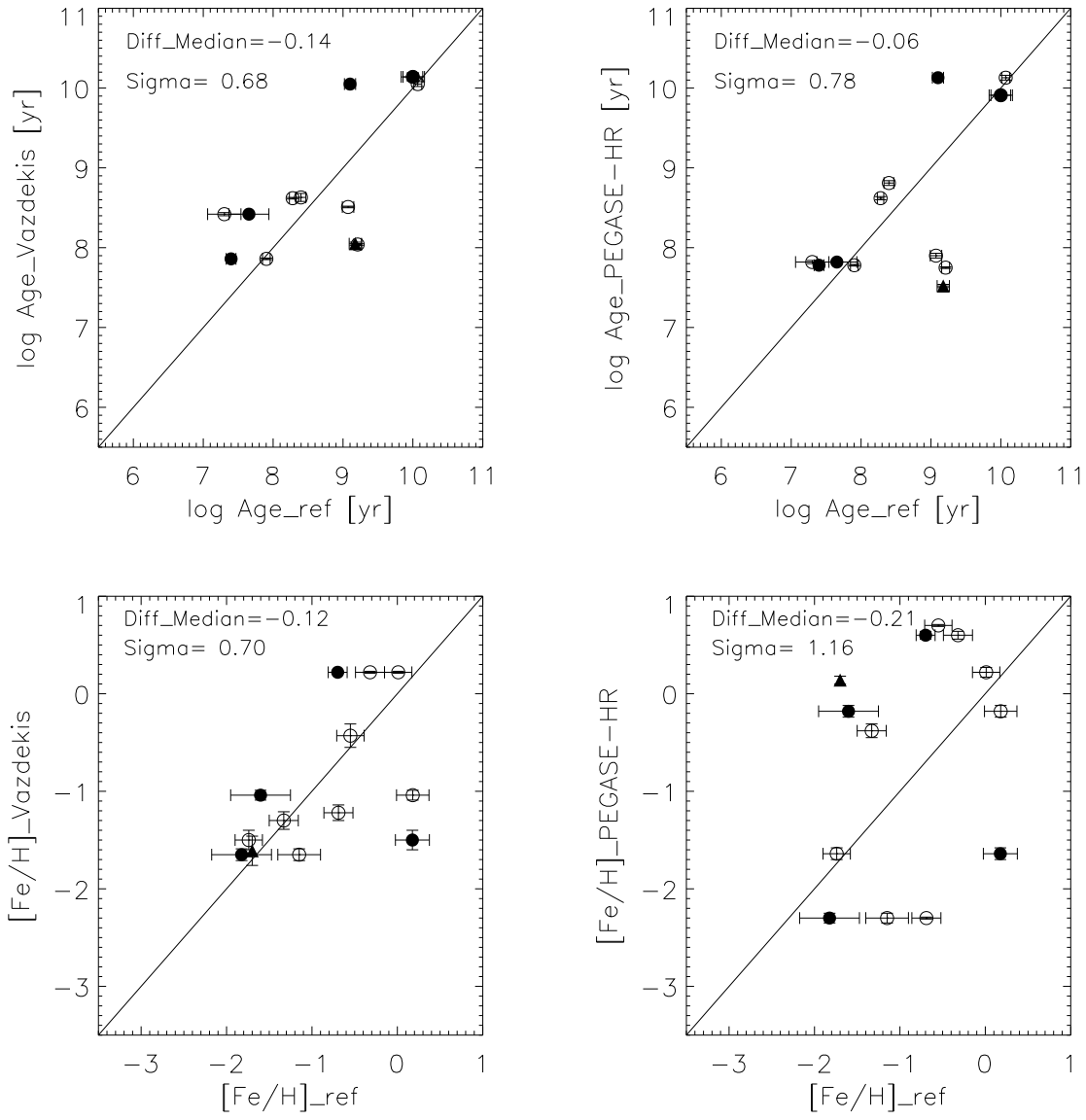


Fig. 4.— Comparisons of the our full-spectrum fitting results of Table 2, ages and metallicities derived with the Vazdekis models (left panels) and PEGASE-HR models (right panels) and those from Beasley et al. (2015) (open circles), Fan et al. (2014) (filled circles) and Sharina et al. (2010) (filled triangles).

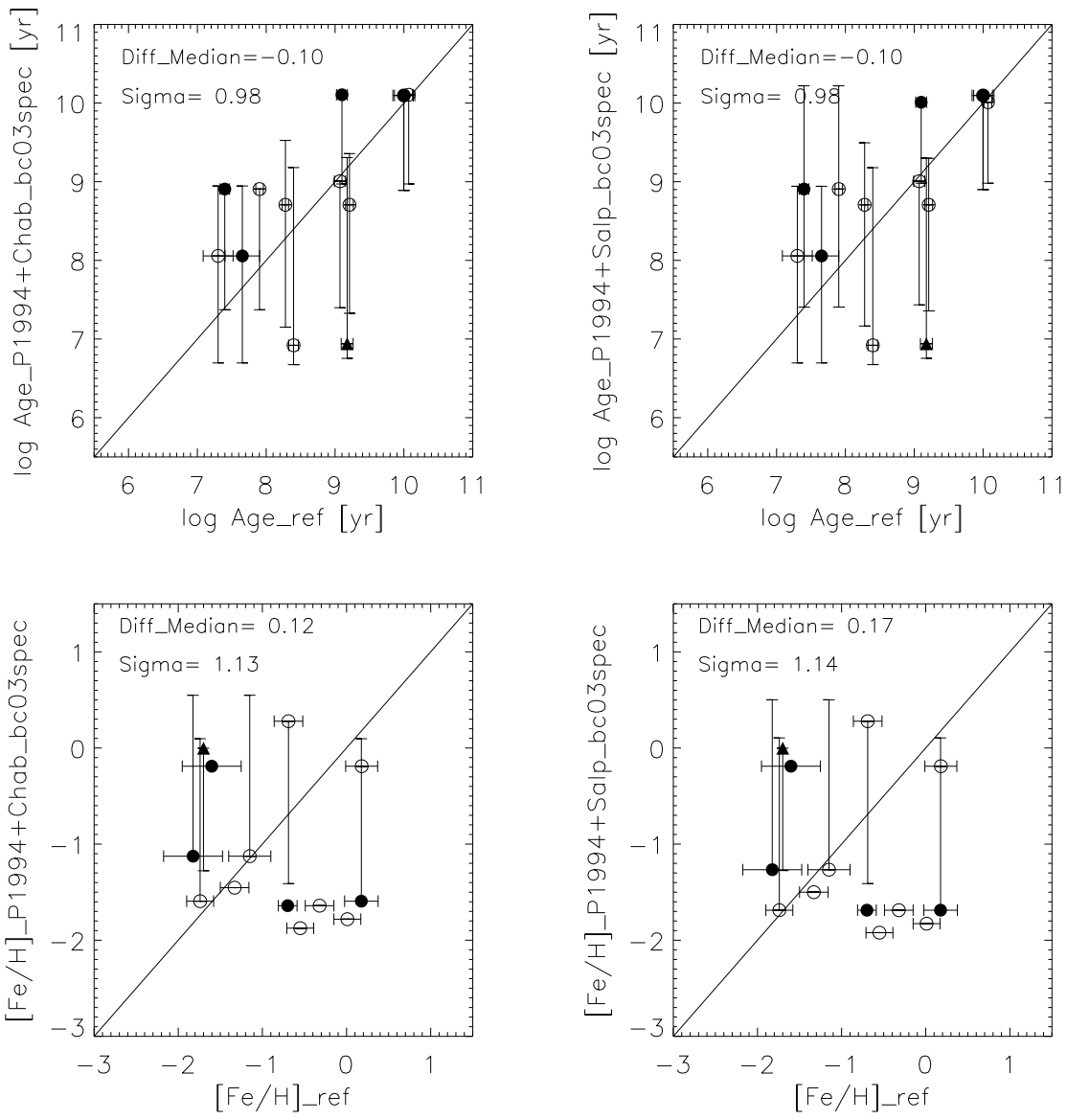


Fig. 5.— Same as Figure 3, fitting only with spectroscopy, but with P1994 tracks + Chabrier (2003) IMF (left panels) and Salpeter (1955) IMF (right panels). The open circles are from Beasley et al. (2015), the filled circles are from Fan et al. (2014) and the filled triangles are from Sharina et al. (2010).

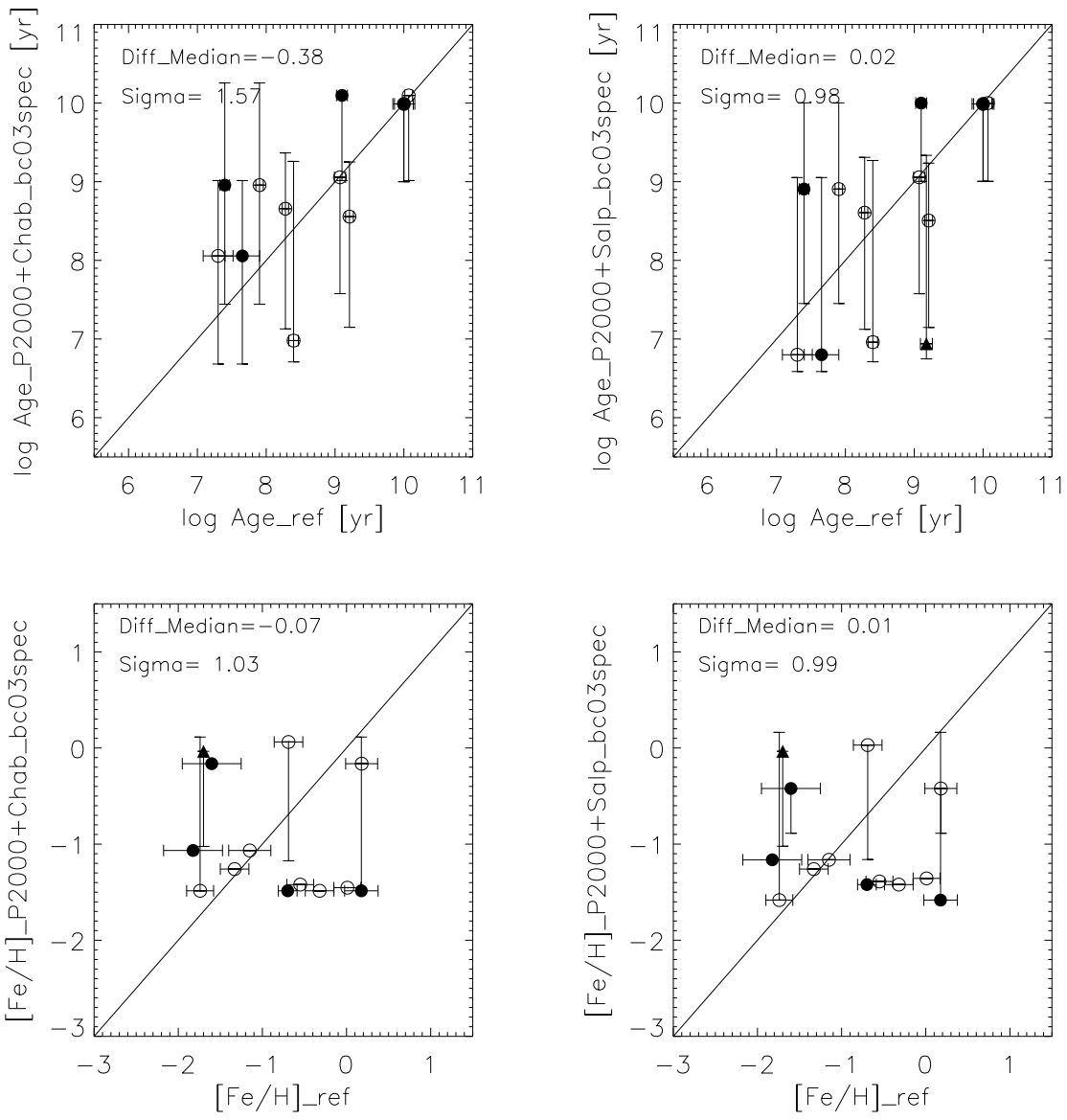


Fig. 6.— Same as Figure 3, fitting only with spectroscopy. The model applied is the Padova 2000 tracks + Chabrier (2003) IMF (left panels) and Salpeter (1955) IMF (right panels). The open circles are from Beasley et al. (2015), the filled circles are from Fan et al. (2014) and the filled triangles are from Sharina et al. (2010).

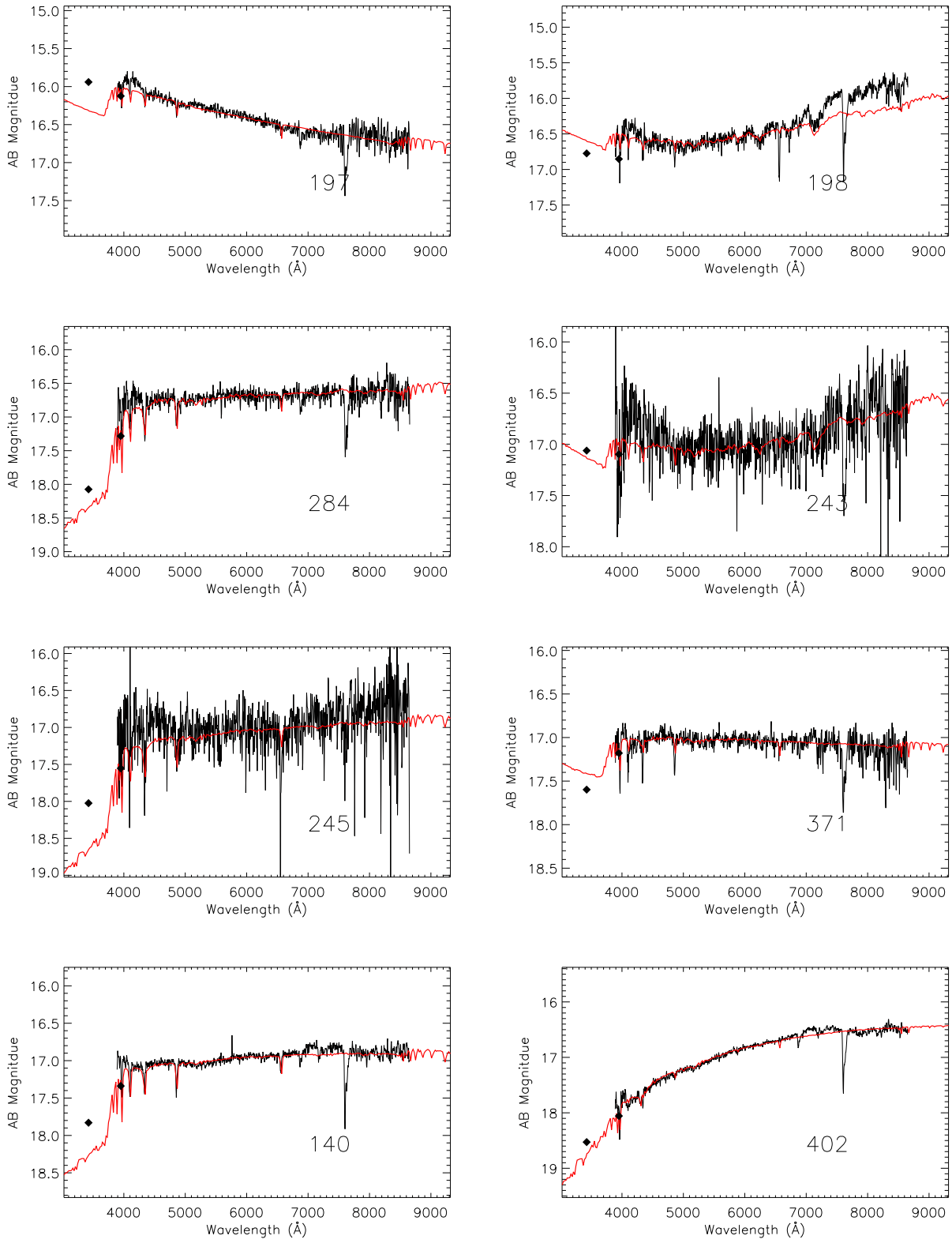


Fig. 7.— SEDs of our sample star clusters in M33. Fitting with spectroscopy and the only photometry from SAGE u_{SC} and v_{SAGE}. The BC03 models with Chabrier (2003) IMF and Padova 2000 tracks are applied for the fitting.

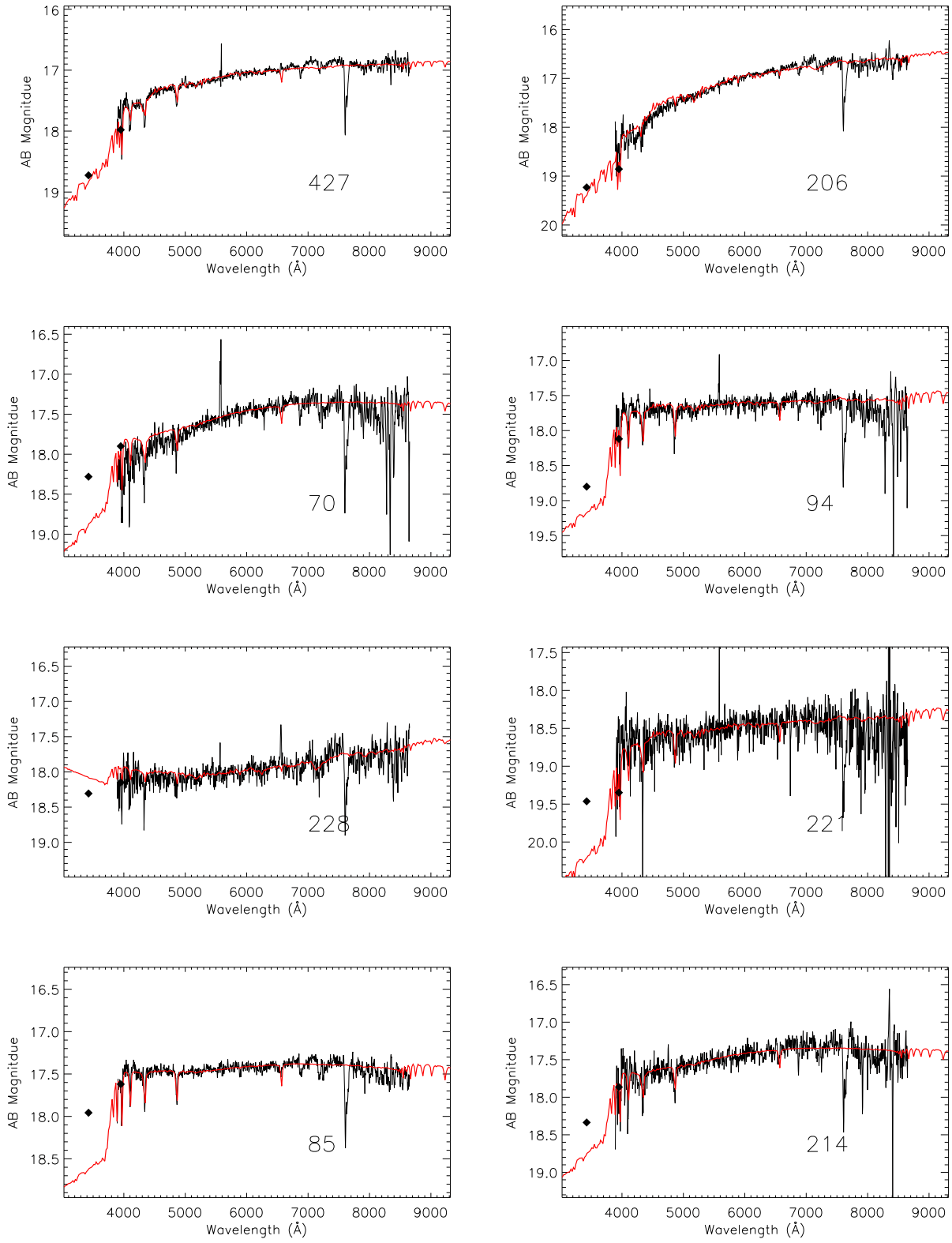


Fig. 8.— -Continued.

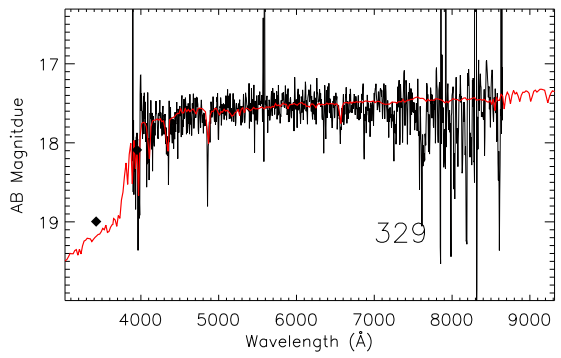


Fig. 9.— -Continued.

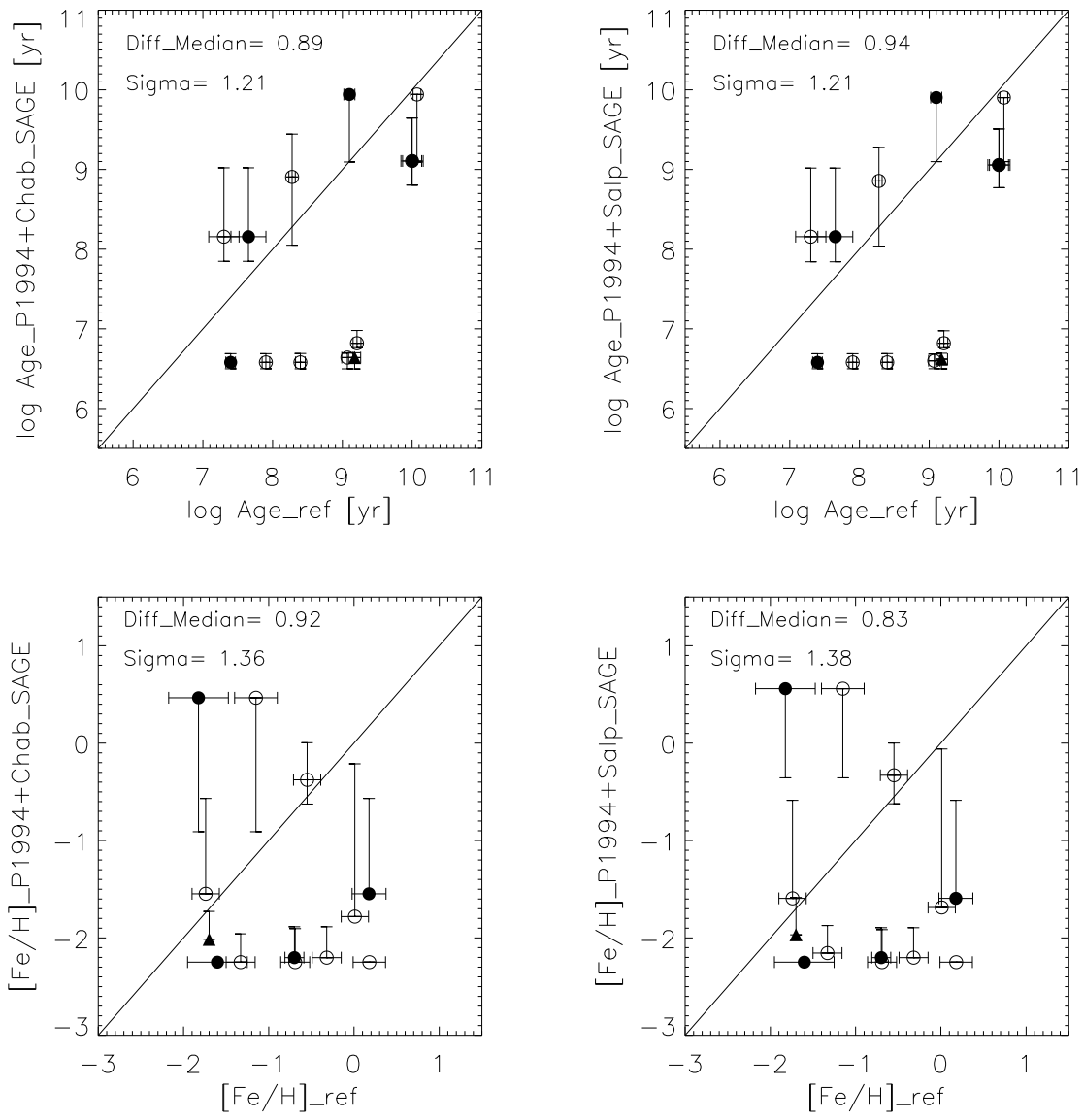


Fig. 10.— Same as Figure 7 but only using the SAGE u_{SC} and v_{SAGE} photometry. The model applied is the Padova 1994 + Chabrier (2003) IMF (left panels) and Salpeter (1955) IMF (right panels) and those from Beasley et al. (2015) (open circles), the filled circles are from Fan et al. (2014) and the filled triangles are from Sharina et al. (2010).

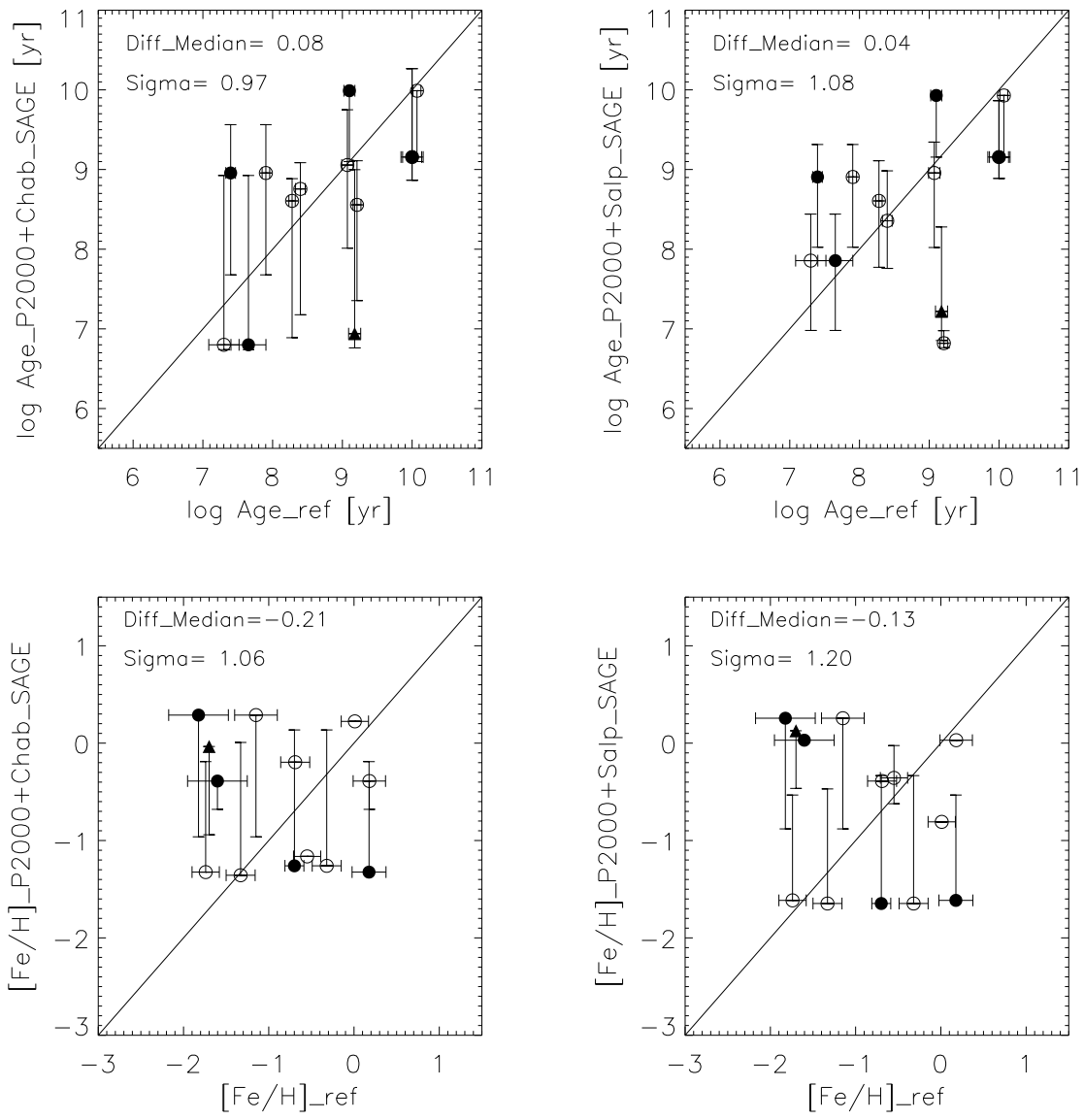


Fig. 11.— Same as Figure 7 but only using the SAGE u_{SC} and v_{SAGE} photometry. The model applied is the Padova 2000 + Chabrier (2003) IMF (left panels) and Salpeter (1955) IMF (right panels) and those from Beasley et al. (2015) (open circles), the filled circles are from Fan et al. (2014) and the filled triangles are from Sharina et al. (2010).

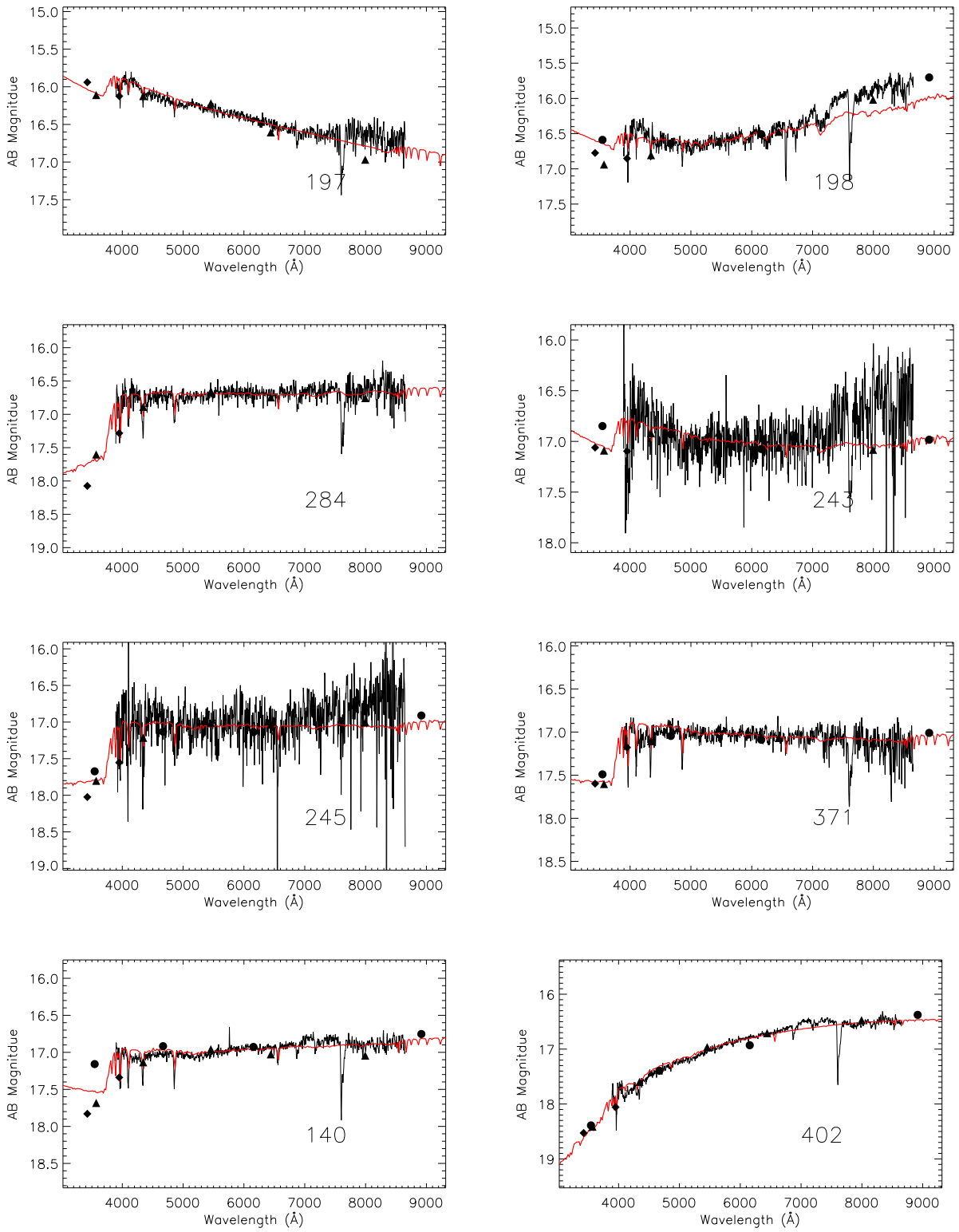


Fig. 12.— Same as in Figure 6 but for spectroscopy and photometry from SAGE u_{SC} and v_{SAGE}, UBVRI and ugriz. The Bruzual & Charlot (2003) models with Chabrier (2003) IMF and Padova 2000 tracks are applied for the fitting. The filled diamonds represent SAGE data; triangles represent UBVRI; filled circles represent ugriz.

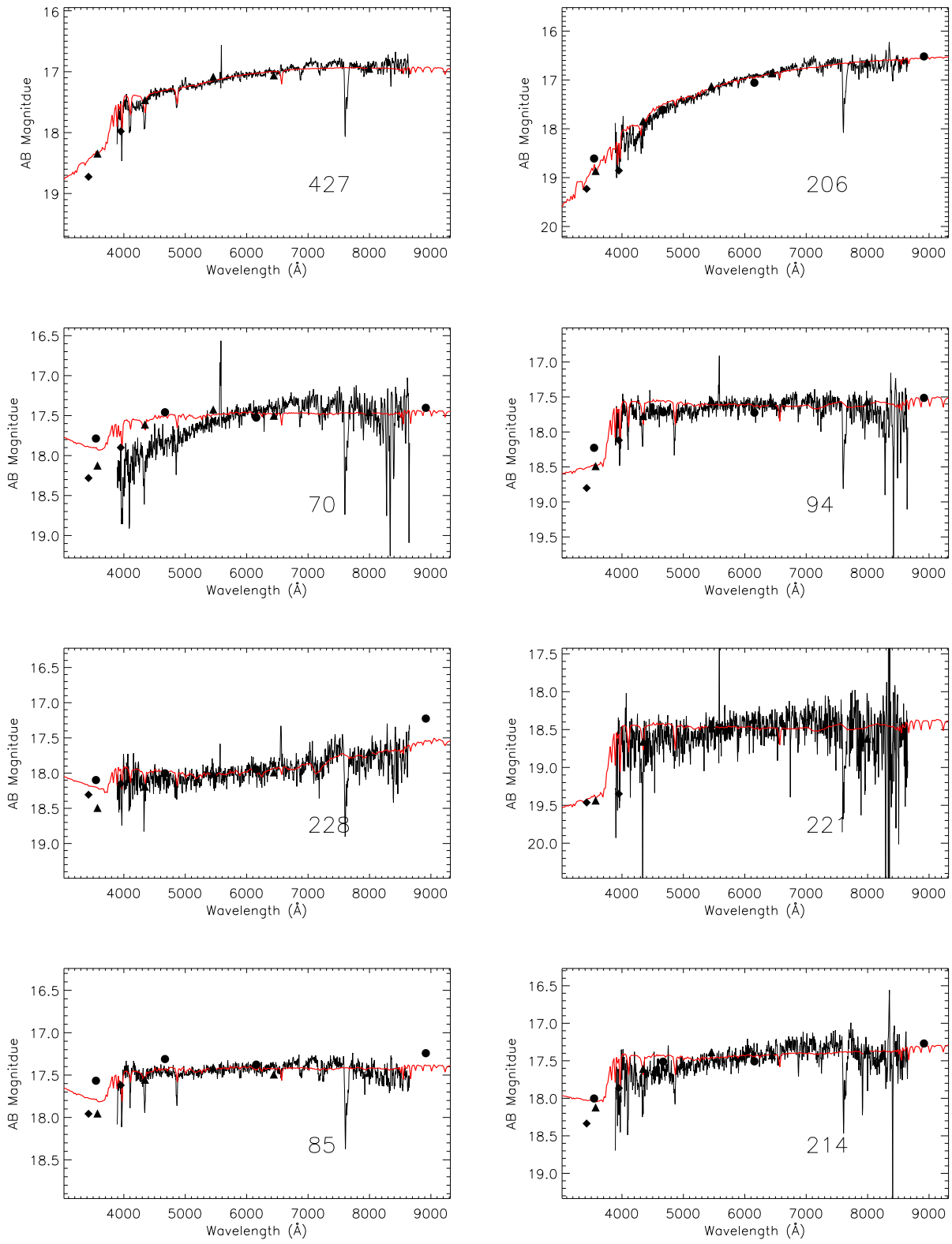


Fig. 13.— -Continued.

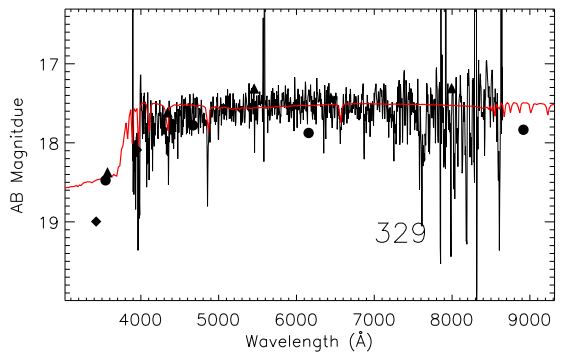


Fig. 14.— -Continued.

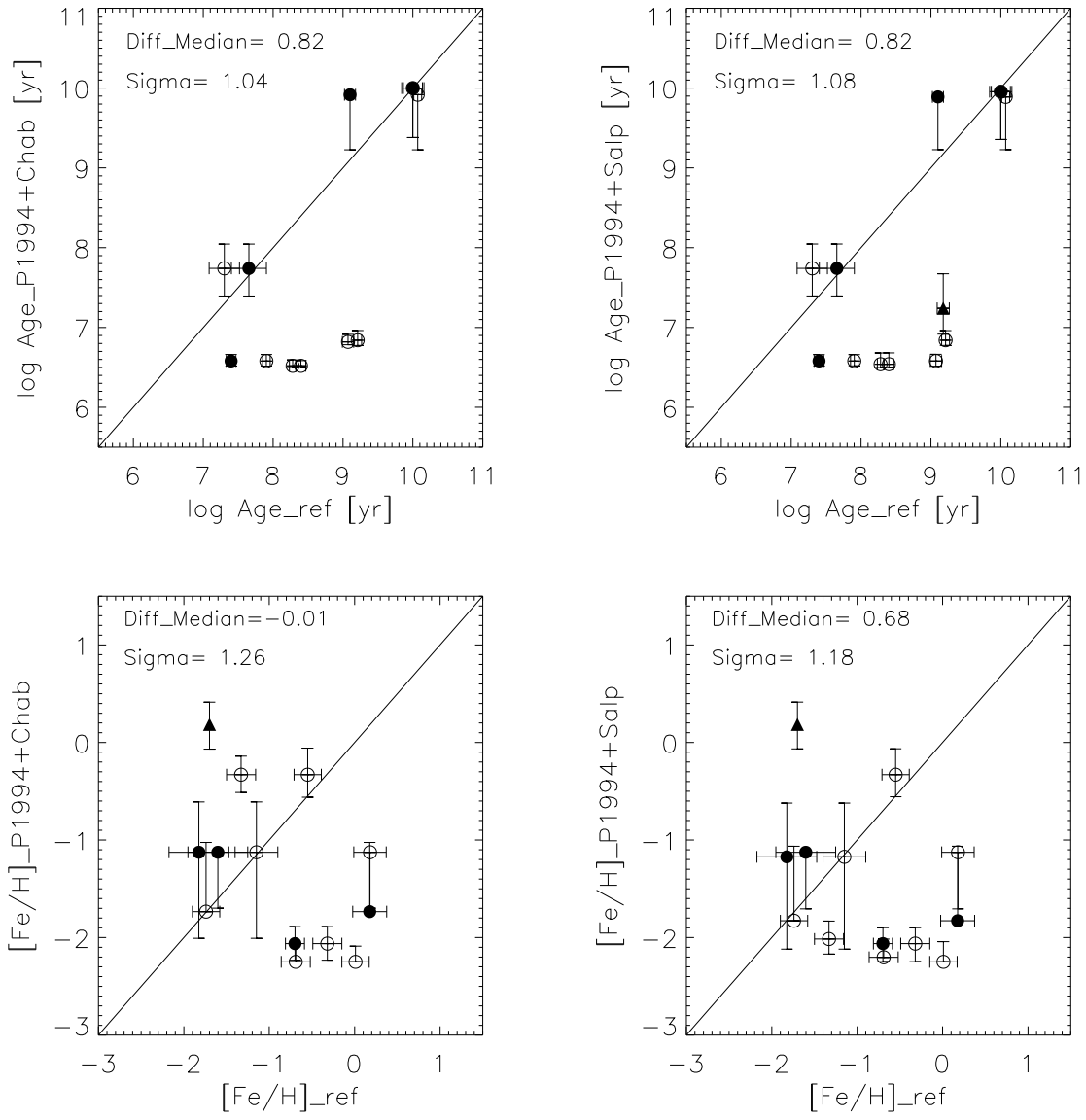


Fig. 15.— Comparisons of the our spectrum-SED fitting results of Table 2, but for the parameters derived with the Padova 1994 track + Chabrier (2003) IMF (left panels) and Salpeter (1955) IMF (right panels) and those from Beasley et al. (2015) (open circles), the filled circles are from Fan et al. (2014) and the filled triangles are from Sharina et al. (2010).

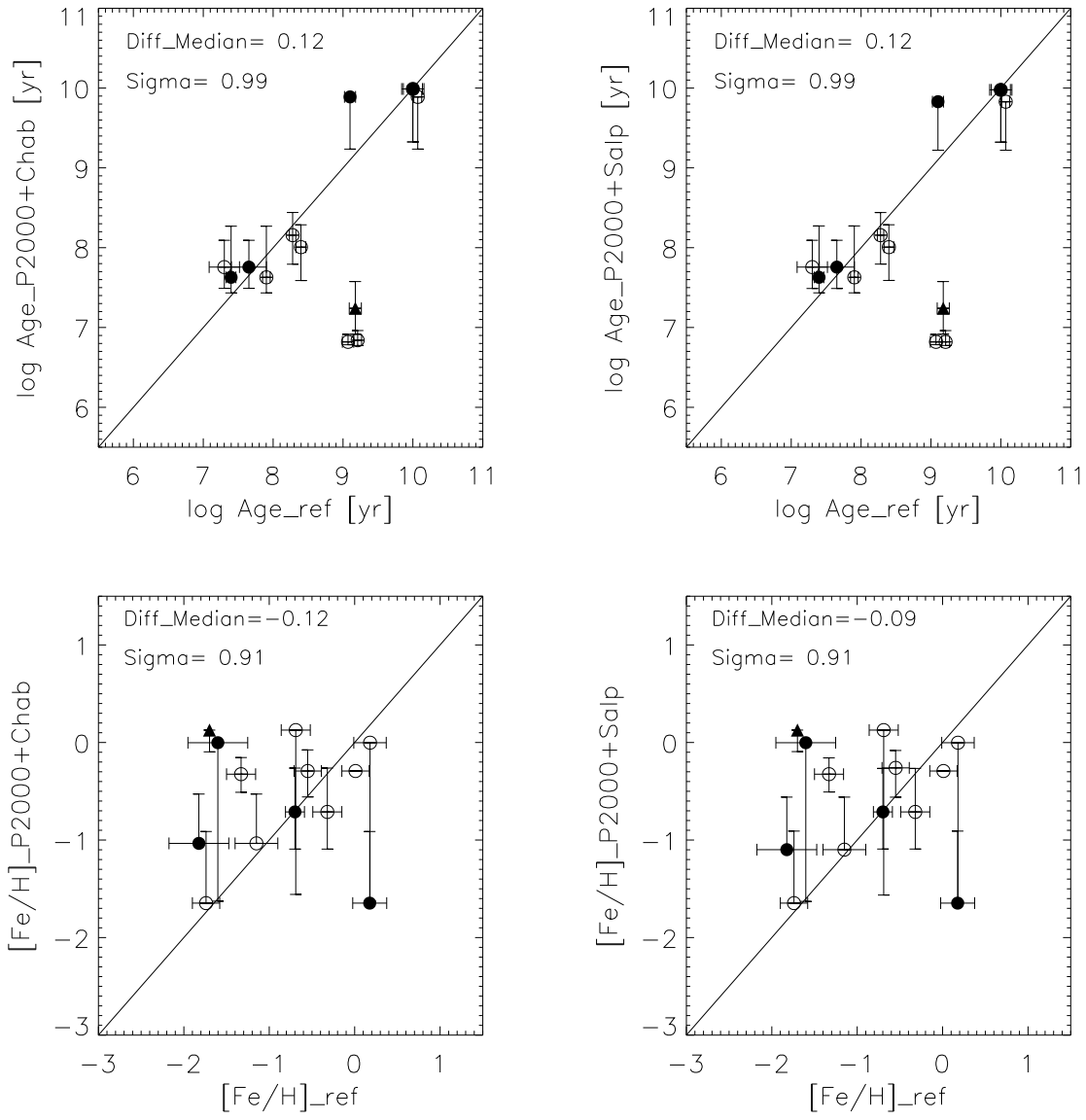


Fig. 16.— Comparisons of the our spectrum-SED fitting results of Table 2, ages and metallicities derived with the Padova 2000 track + Chabrier (2003) IMF (left panels) and Salpeter (1955) IMF (right panels) and those from Beasley et al. (2015) (open circles), the filled circles are from Fan et al. (2014) and the filled triangles are from Sharina et al. (2010).

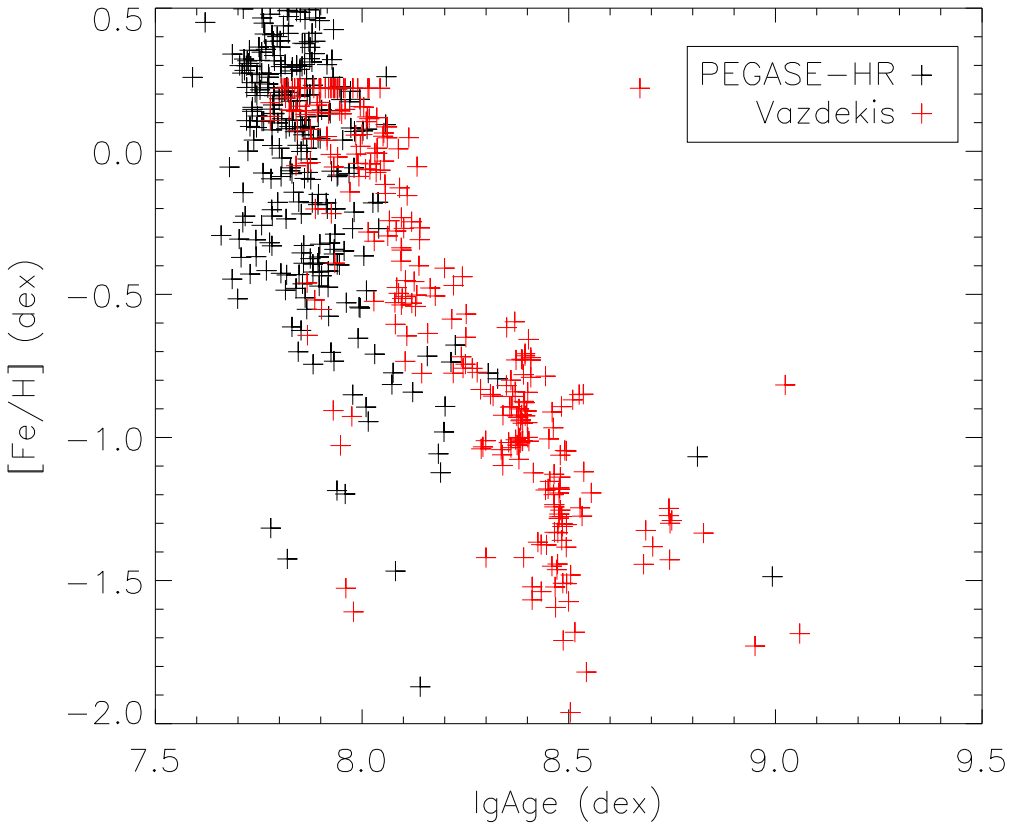


Fig. 17.— The age-metallicity degeneracy testing in our full-spectrum fitting with PEGASE-HR models (black crosses) and Vazdekis models (red crosses).

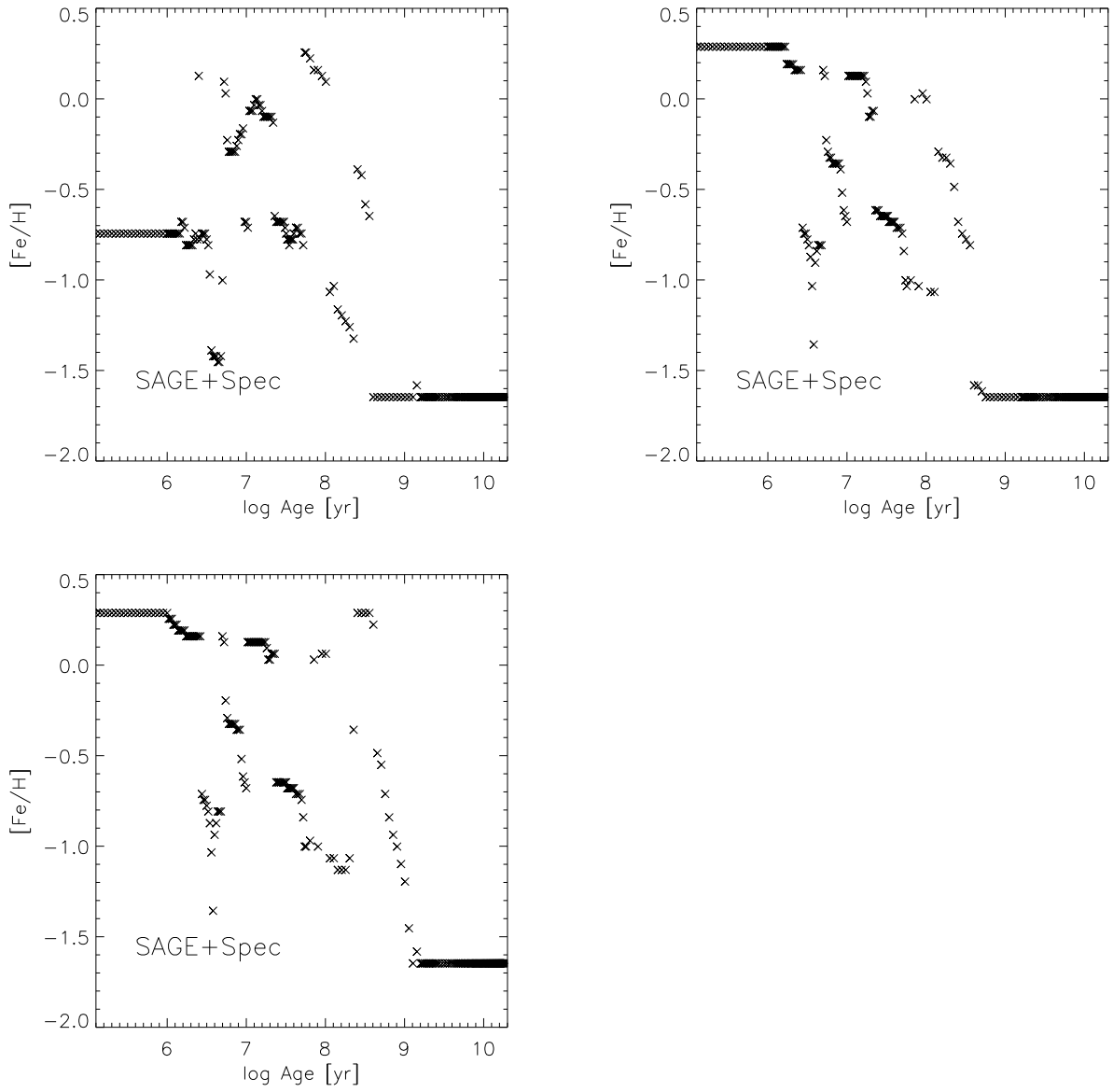


Fig. 18.— The age-metallicity degeneracy testing in our the fitting with Padova 2000 track and Chabrier (2003) IMF of BC03 models. We show the different degeneracy effect in the full-spectrum (top left), SED+spectrum (top right) and SAGE photometry+spectrum(bottom left).

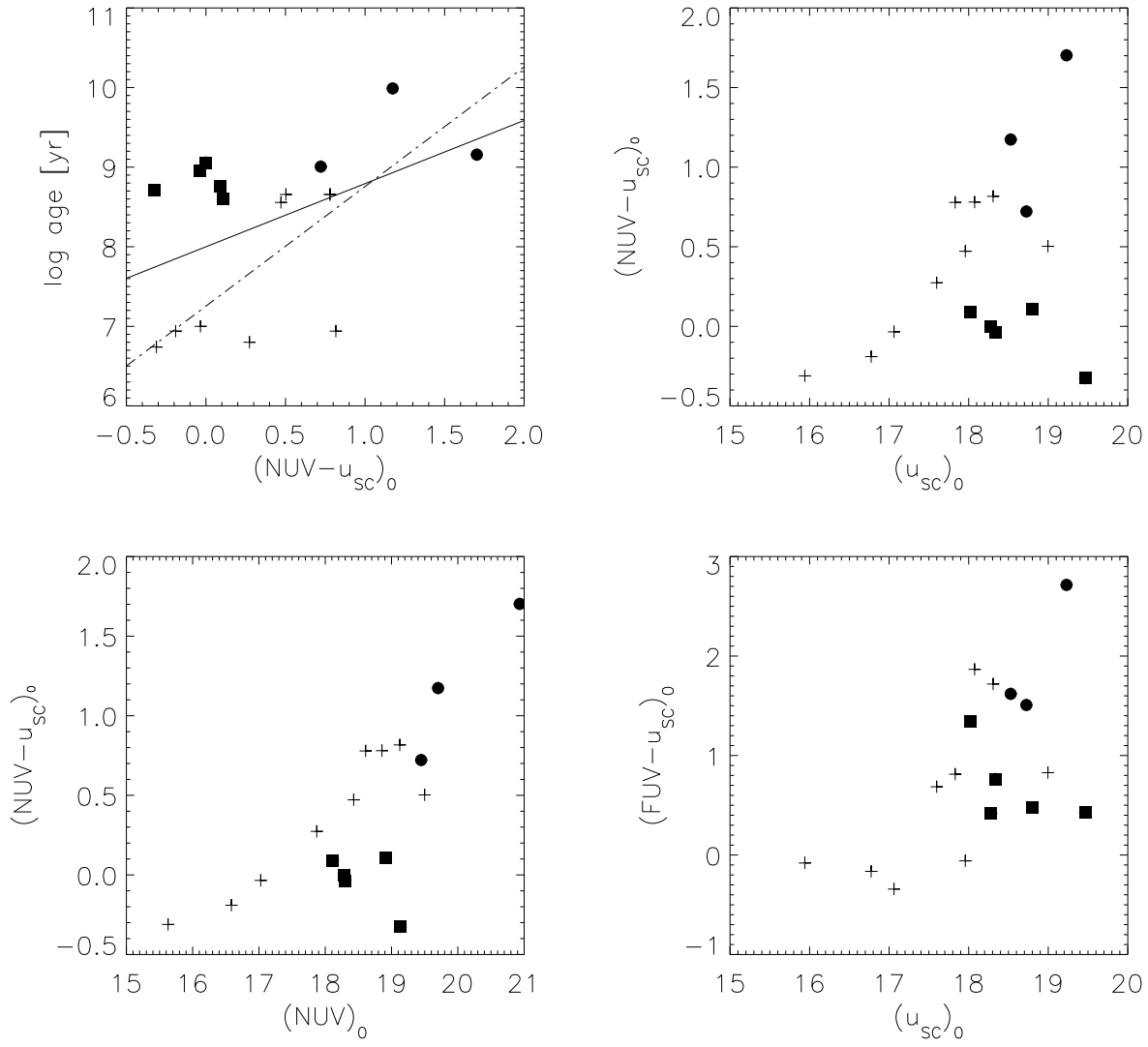


Fig. 19.— *Top left:* The relations between GALEX $(\mathrm{NUV}-\mathrm{u_{SC}})_0$ color and the age (SAGE photometry+observed spectrum, fitted with Padova 2000 evolutinary track and Chabrier (2003) IMF of BC03 models) for our sample star clusters; *Top Right:* $(\mathrm{NUV}-\mathrm{u_{SC}})_0$ color versus SAGE $(\mathrm{u_{SC}})_0$; *Bottom Left:* $(\mathrm{NUV}-\mathrm{u_{SC}})_0$ color versus GALEX NUV_0; *Bottom Right:* GALEX $(\mathrm{FUV}-\mathrm{u_{SC}})_0$ color versus SAGE $(\mathrm{u_{SC}})_0$. The filled circles are clusters older than 1 Gyrs; the black squares (ID: 245, 70, 94, 221 and 214) are further away from the bulk correlation which are considered to be with different characters with the bulk; the rest are crosses. The solid line is the linear fitting for all the data set while the dashed-dotted line is the fitting excluded the five black squares, which improves the correlation coefficients significantly (from 0.44 to 0.76).

.

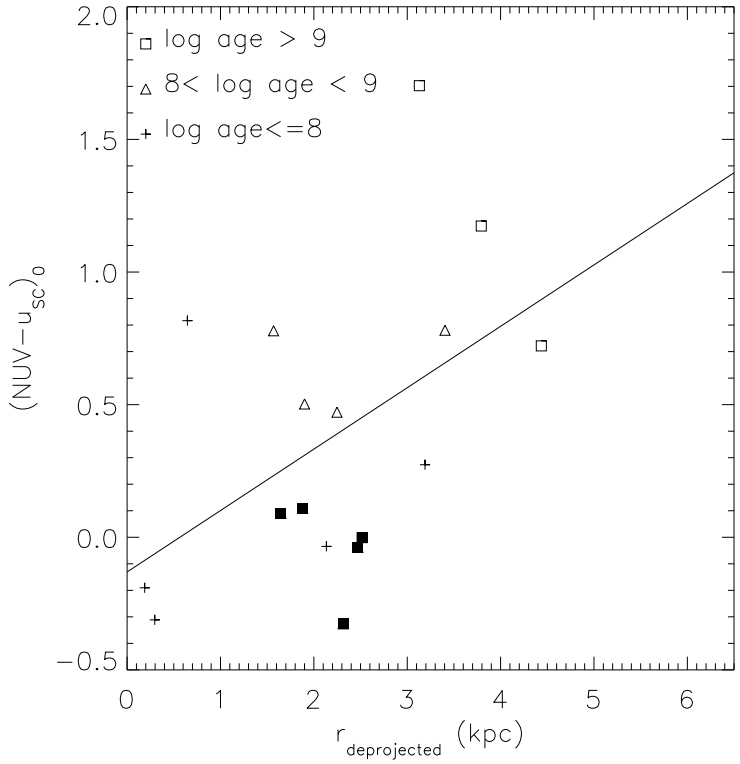
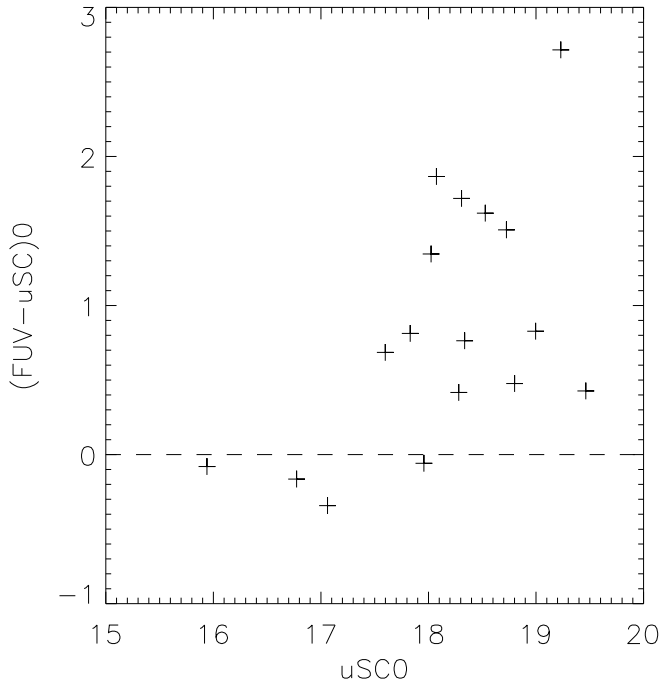
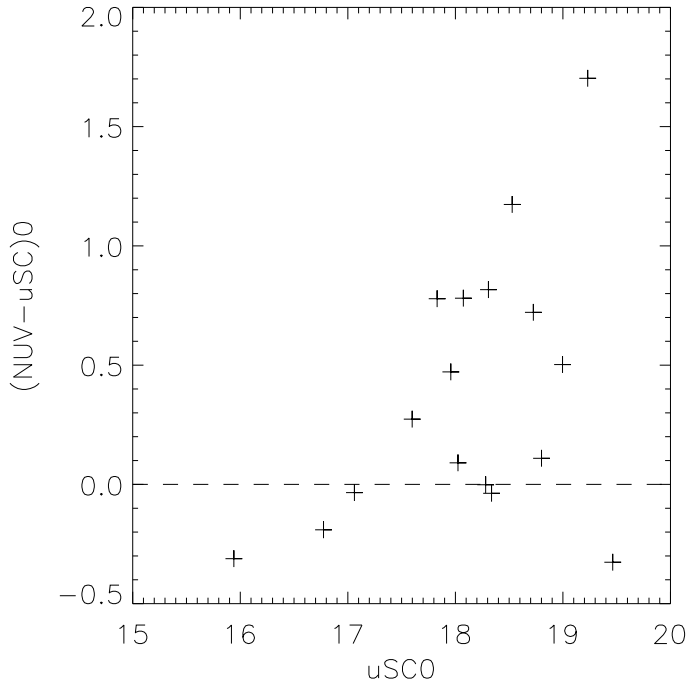
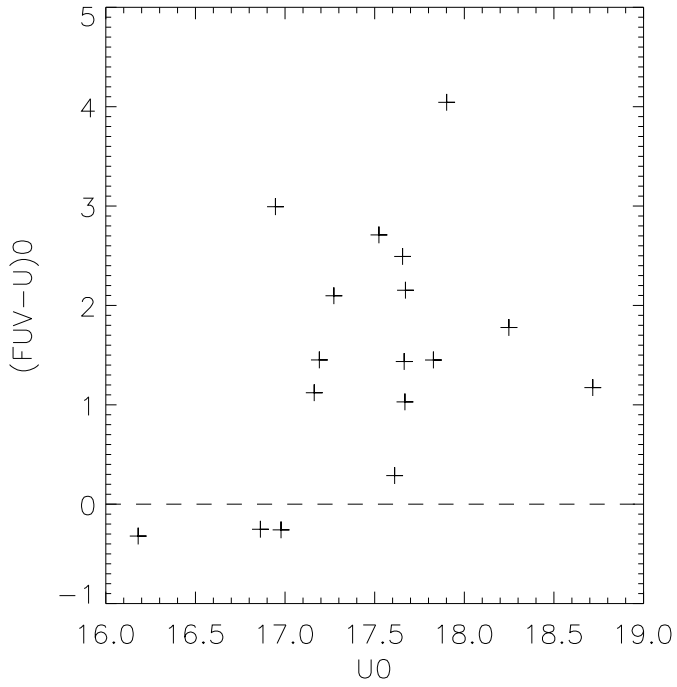


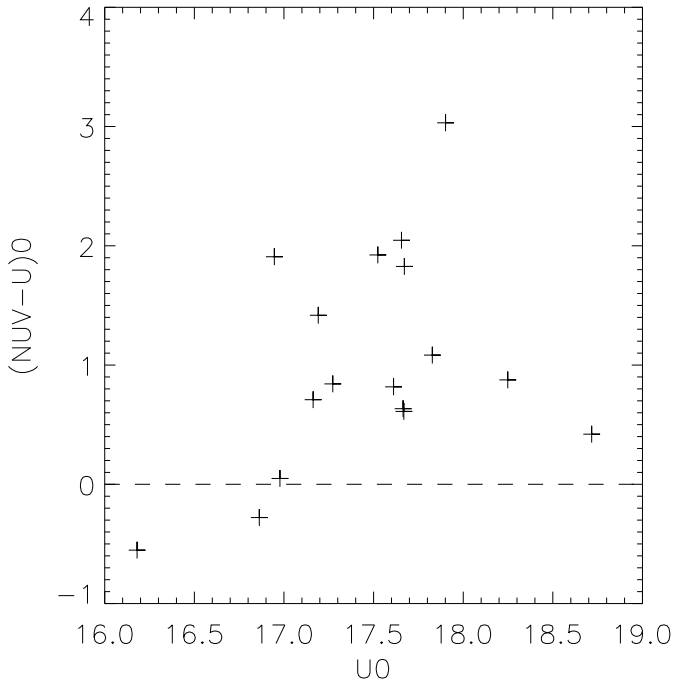
Fig. 20.— The GALEX $(\mathrm{NUV} - \mathrm{u_{SC}})_0$ color versus clusters deprojected distance to M33 center. The sample clusters are shown with different symbols for different age subgroups. The solid line is the linear fitting for all the clusters. The black squares (ID: 245, 70, 94, 221 and 214) are the sources further away from the bulk correlation in Figure 19

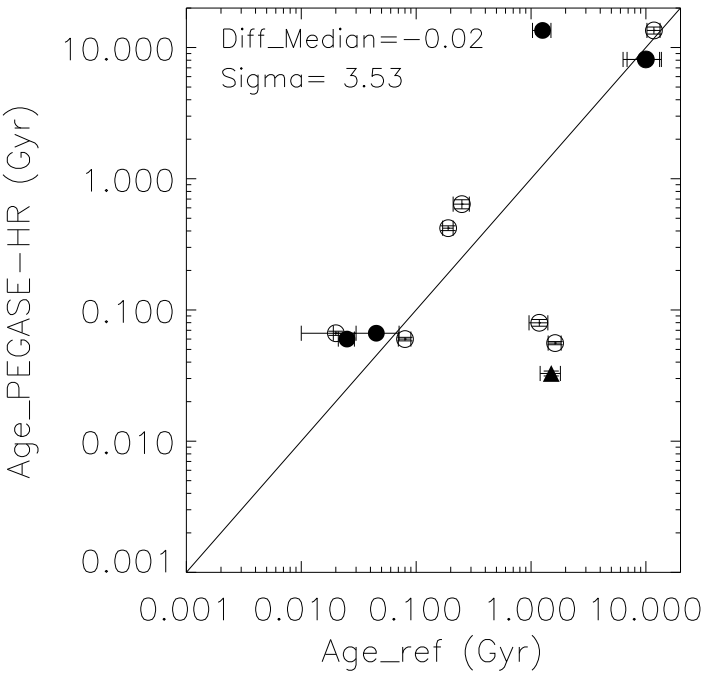
.

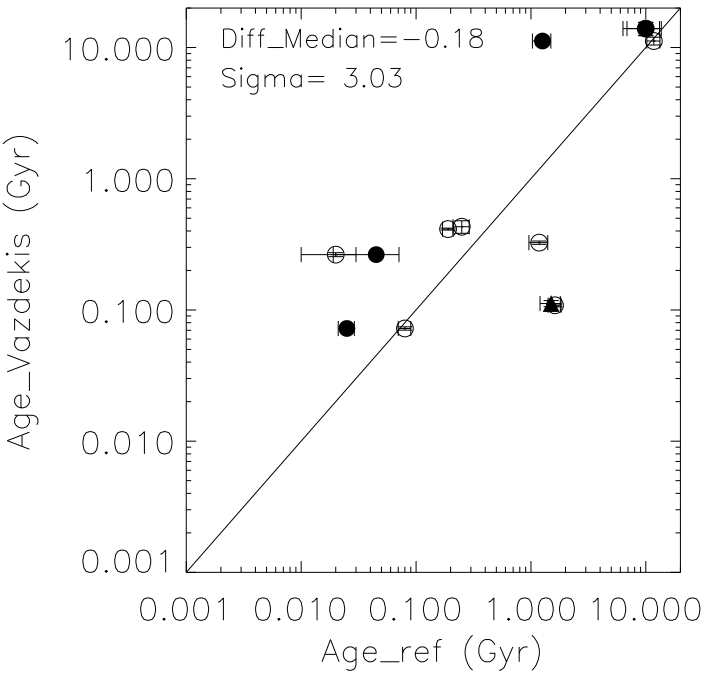

(FUV−uSC)0
uSC0
3
2
1
0
−1
15
16
17
18
19
20

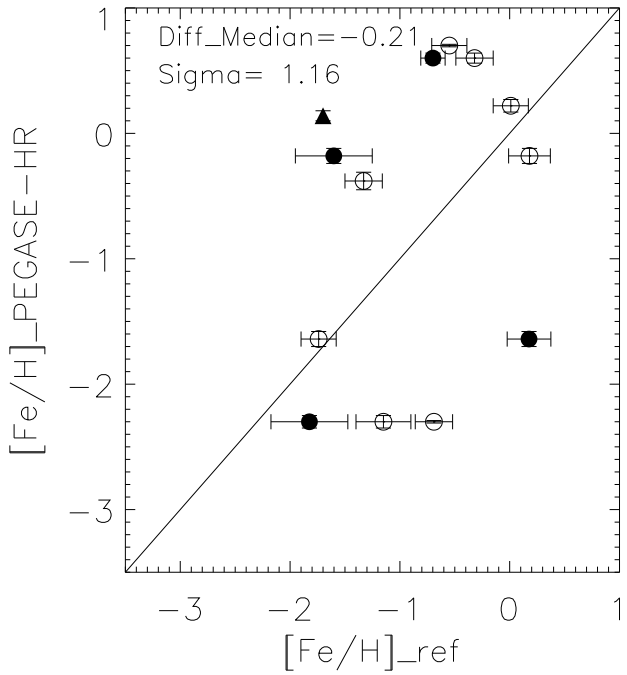

(NUV−uSC)0
uSC0
2.0
1.5
1.0
0.5
0.0
−0.5
15
16
17
18
19
20

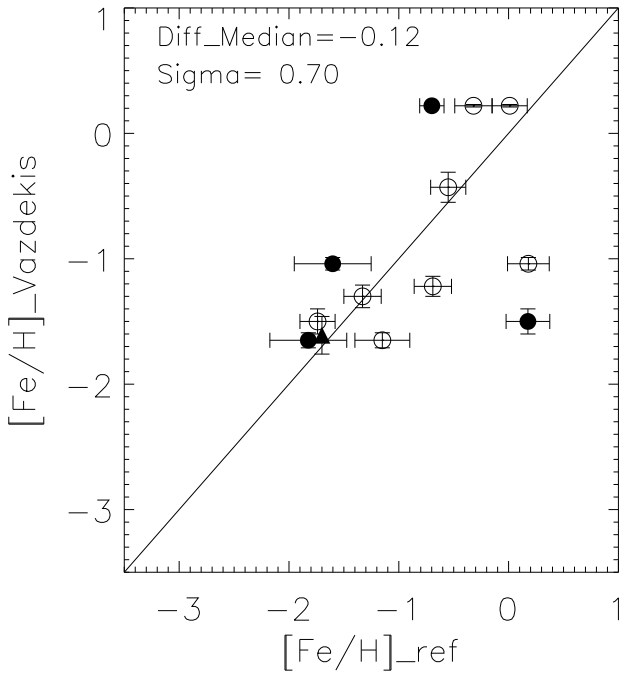

(FUV−U)0
U0
5
4
3
2
1
0
−1
16.0
16.5
17.0
17.5
18.0
18.5
19.0


(NUV−U)0
U0
4
3
2
1
0
−1
16.0
16.5
17.0
17.5
18.0
18.5
19.0


Diff_Median=−0.02
Sigma= 3.53
Age_PEGASE−HR (Gyr)
Age_ref (Gyr)
10.000
1.000
0.100
0.010
0.001
0.001 0.010 0.100 1.000 10.000


Diff_Median=−0.18
Sigma= 3.03
Age_Vazdekis (Gyr)
Age_ref (Gyr)
10.000
1.000
0.100
0.010
0.001
0.001 0.010 0.100 1.000 10.000


Diff_Median=−0.21
Sigma= 1.16
[Fe/H]_PEGASE−HR
[Fe/H]_ref
1
0
−1
−2
−3
−3 −2 −1 0 1


Diff_Median=−0.12
Sigma= 0.70
[Fe/H]_Vazdekis
[Fe/H]_ref
1
0
−1
−2
−3
−3 −2 −1 0 1